VALIDATION OF CANDIDATE GENES IN RESPONSE TO VERSICAN MANIPULATION IN DEVELOPING SYNOVIAL JOINTS

by

Stephen Ryan Vick

June 22nd, 2012

Director: Dr. Anthony Capehart

Major Department: Biology

Little is understood about the complex process of synovial joint formation in early limb development. It has been shown that versican is highly expressed in the extracellular matrix of these joints (Snow et al., 2005; Shepard et al., 2007) and the knockdown of versican leads to malformation of the interzone, tissues that form the articular cartilage and synovial cavity (Nagchowdhuri et al., 2012). It is also thought that these effects impact gene expression in cells that are involved in the developing joint.

Versican is chondroitin sulfate proteoglycan. It has four functional-modules: the N-terminal domain, the C-terminal domain, and GAG-α, and GAG-β chondroitin sulfate attachment regions. The N-terminal domain is also known as the G1 domain and the C-terminal domain is also known as the G3 domain (Kimata et al., 1986 and Zimmerman et al., 1989).

In previous studies versican protein expression has been reduced and the G1 domain has been over-expressed to observe how these changes in the developing joint tissue effect gene expression. This study is a validation of microarray data specifically focusing on hyaluronan and Wnt pathway genes as they pertain to the misexpression of versican.

RT-PCR and real-time PCR were used in this study to validate expression of the genes chosen. Through the use of these techniques the degree of expression has been quantified and compared to the fold changes observed with the microarray data. Overall, G1 versican mediated gene expression in the developing joint with regard to hyaluronan and Wnt pathway transcript regulation were in agreement with results obtained by RNA array.

VALIDATION OF CANDIDATE GENES IN RESPONSE TO VERSICAN MANIPULATION IN DEVELOPING SYNOVIAL JOINTS

A Thesis

Presented to

The Faculty of the Department of Biology

East Carolina University

In Partial Fulfillment

Of the Requirements for the Degree

Masters of Science in Molecular Biology

by

Stephen Ryan Vick

June 22nd, 2012

VALIDATION OF CANDIDATE GENES IN RESPONSE TO VERSICAN MANIPULATION IN DEVELOPING SYNOVIAL JOINTS

By

Stephen Ryan Vick

APPROVED BY:

DIRECTOR OF THESIS: _____

Anthony Capehart, Ph.D

COMMITTEE MEMBER:_____

Jean-Luc Scemama, Ph.D

COMMITTEE MEMBER:_____

Baohang Zhang, Ph.D

COMMITTEE MEMBER:_____

John Wiley, Ph.D

CHAIR OF THE DEPARTMENT OF BIOLOGY:_____

Jeff McKinnon, Ph.D

DEAN OF THE GRADUATE SCHOOL:_____

Paul Gemperline, Ph.D

ACKNOWLEDGMENTS

I would like to thank Dr. Capehart for allowing me to work and earn my degree in his lab. His patience and guidance through my work was greatly appreciated and made me into a better student and also a better scientist.

I would also like to thank my committee members: Dr. Baohang Zhang, Dr. Jean-Luc Scemama, and Dr. John Wiley. They answered countless questions dealing with my project over the last two years. The resources and time they provided were unmatched and immensely appreciated.

The small group of students that I became very close with in my time in the department also played a critical role in my development as a scientist. Christine Basham, Sarah Thalhamer, and Eli Robins were there every day to answer questions, share a meal, or lend an ear. They made the transition to graduate student a lot easier and I will always thank them for that.

Finally, I would like to thank my family for all of their love and support through this time in my life. My wife, Amanda Vick, was the unwavering support system during the last two years. My parents, Stephen and Jamie Vick, supplied countless advice and prayers that will always be remembered. Thank you for all that you have done to make me the man I am today. I love you.

Table of Contents

List of Tables

List of Figures

1. Introduction

LIMB DEVELOPMENT

The limb develops along three axes: proximal-distal anterior-posterior and dorsal-ventral. Limb development begins in the limb field, the region where the limb bud forms. The limb bud is first represented as a bulge of cells that occurs when mesenchyme cells begin to aggregate underneath the ectodermal tissue. In vertebrates there are only four limb buds per embryo, with respect to the midline (Gilbert 2006).

When mesenchyme cells enter the limb field they secrete Fgf10, a type of fibroblast growth factor, which induces the formation of the apical ectodermal ridge (AER) (Gilbert 2006, Ohuchi 1997). The expression of Wnt2b in the forelimb and Wnt8c in the hindlimb stabilizes the signaling of Fgf10, so that it remains localized in these regions of the lateral plate mesoderm. The AER extends along the distal margin of the developing limb and eventually becomes a major signaling center for the developing limb (Gilbert 2006). At the same time the AER secretes Fgf8 which stimulates mitosis in mesenchyme cells and causes continued expression of Fgf10; therefore a positive feedback system is established- in which Fgf10 induces formation of the AER and the AER secretes Fgf8 to continue expression of Fgf10 (Gilbert 2006).

The anterior-posterior axis of the developing limb is established by signals from mesenchyme cells in the zone of polarizing activity. The major signal secreted from the zone of polarizing activity is transcribed from the sonic hedgehog (shh) gene. Sonic hedgehog expression is observed in more distal regions of the developing limbs and gives rise to the development of the digits.

The third axis of the developing limb, the dorsal-ventral axis, is organized by the non-ridge ectoderm and the gene particularly important in this development is Wnt7a. Wnt7a expression is needed for dorsal patterning of the limb (Gilbert 2006) because when Wnt7a is knocked out in mice ventral characteristic pads develop on the dorsal and ventral side of the paw (Parr and McMahon 1995).

Wnt also signaling remains as an important regulator of subsequent stages of limb development through both canonical and non-canonical pathways. Non-canonical Wnt signaling can be divided into two sub categories: the planar cell polarity (PCP) pathway and the Wnt/Ca^{+2} pathway (Komiya et al., 2008). The PCP pathway plays a role in the organization of the actin cytoskeleton and can impact cellular movement and structure (Komiya et al., 2008). This PCP mechanism may govern cellular polarity in growth plate chondrocytes, properly aligning cells for division and growth of the bone in length (Li and Dudley, 2009). Studies have shown that through loss- and gain-of-function experiments with Wnt/PCP pathway components (Fzd7 and Vangl2), that proliferative chondrocytes show defects in their orientation, ultimately resulting in defects in skeletal development (Li and Dudley, 2009).

Figure 1. Schematic of Wnt/PCP Pathway

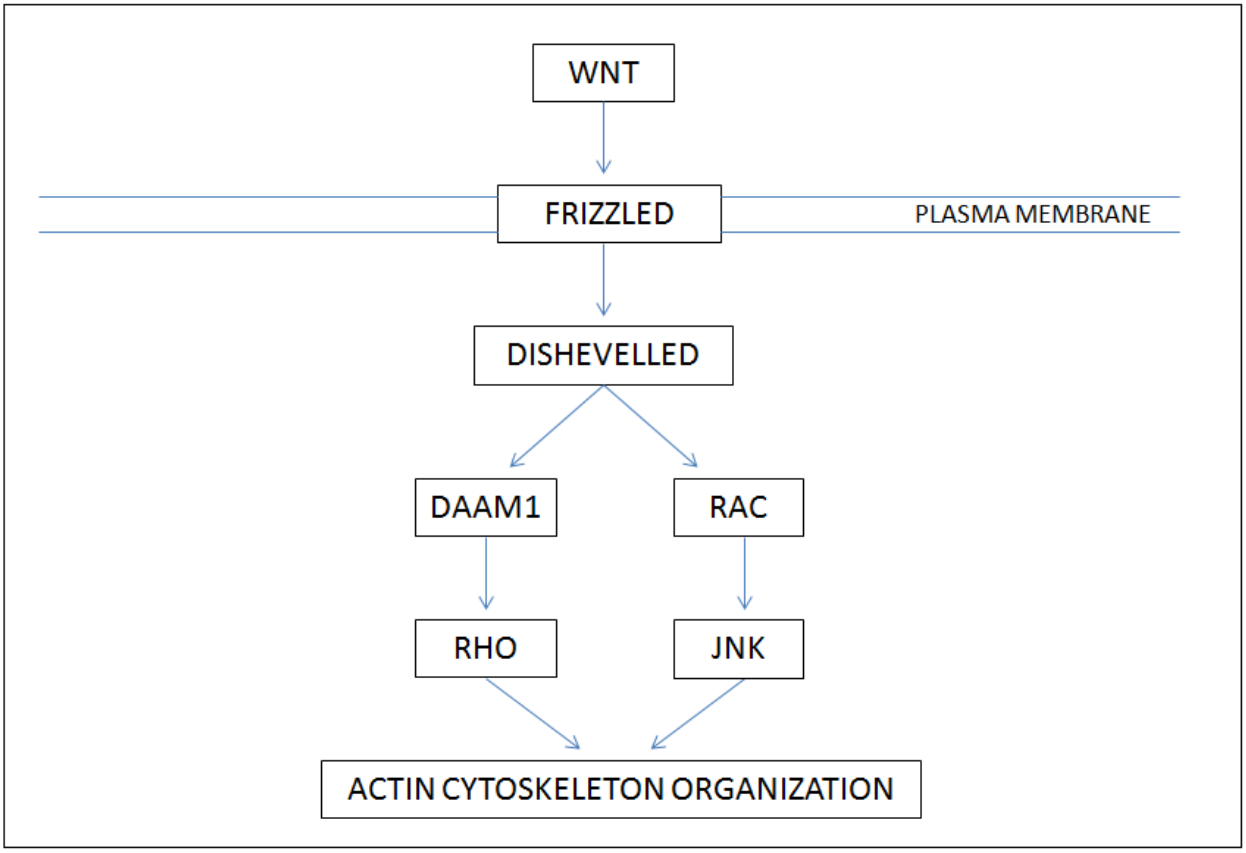

Figure 1. A schematic depicting noncanonical Wnt/PCP signaling in the cell (Modified from Habas 2005).

JOINT DEVELOPMENT

As the limb develops; the elbow joint forms where the prospective humerus, radius, and ulna intersect to form a Y-shaped cartilaginous structure. Joint formation begins with the formation of the interzone, an area that includes the eventual synovial cavity and articular cartilages of the proximal ends of the radius and ulna, and distal end of the humerus. The interzone is comprised of tightly-packed mesenchymal cells and in avian joints the interzone is usually thicker than mammalian joints (Pacifici et al., 2005). There is not much known about the function of the interzone, but it is believed that interzone cells are responsible for the formation of other joint tissues and structures (Pacifici et al., 2005).

It has been shown that the canonical Wnt/β-catenin signaling pathway is both sufficient and necessary for the induction of synovial joints in the developing chick limb. This indicates that Wnt/β-catenin may act at initial steps of the regulatory hierarchy in synovial joint formation (Guo 2004). Wnt4, Wnt9a, and Wnt16 are expressed in the forming joint in overlapping and complementary patterns, and may play redundant roles in activating β-catenin and joint formation (Guo 2004). Expression of these genes in the presumptive joint results in up-regulation of β-catenin and inhibition of Sox9, which leads to the induction of synovial joint formation (Guo 2004). Sox9 has been seen as an activator of collagen type II, which is a gene encoding a major structural component of cartilage (Bell 1997; Ng 1997). The first step of this induction by Wnt signaling is formation of interzone cells by inhibiting chondrocyte differentiation and inducing growth/differentiation factor 5 (Gdf5) expressions (Guo 2004, Hartmann 2000). Gdf5 promotes the initiation of chondrogenesis, chondrocyte proliferation (Francis-West et al., 1999), and helps to maintain the joint in early stages of development (Storm and Kingsley, 1999).

Once the interzone is established cavitation and morphogenesis occur, which is the physical separation of the two opposing sides of the developing synovial joint and formation of the interlocking structures of the joint, respectively. It is believed that the glycosaminoglycan, hyaluronan, is involved in cavitation. Synthesis and accumulation of hyaluronan contributes to the breakdown of tissues in the interzone, leading to the physical separation of the opposing ends of the skeletal template and formation of the fluid filled cavity (Pacifici et al., 2005). Once cavitation occurs the morphogenetic processes begin to mold the opposing sides of the joint into reciprocally-shaped and interlocking structures. These morphogenetic processes occur over a considerable amount of developmental time and eventually lead to maturation of the joint in which the proximal end and the distal end are separated by a fluid filled synovial cavity (Pacifici et al., 2005).

VERSICAN

Versican, a chondroitn sulfate proteoglycan of the hyalectin family, is highly expressed in the extracellular matrix of developing synovial joints (Snow et al., 2005; Shepard et al., 2007).. A proteoglycan is a glycoprotein bearing covalently attached glycosaminoglycans (GAGs), and chondroitin sulfate is a long unbranched sulfated GAG consisting of repeating disaccharide units of glucoronate and N-acetylgalactosamine. Like other members of the hyalectin family, versican is a modular molecule, meaning that it is composed of different functional domains (Shinomura et al., 1993).

There are three functional domains in the core protein of versican: the G1, GAGα, GAGβ, and G3. The G2 domain is made up of two exons that contain chondroitin sulfate attachment regions, GAG-α and GAG-β (Fig 7) (Wight 2002). The G1 domain is the N-terminus, which binds to hyaluronan, and the G3 domain is the C-terminus (Kimata et al., 1986; Zimmerman et al., 1989). The binding of the G1 domain and hyaluronan may be stabilized by linkprotein (Matsumoto et al., 2003). The G3 domain has a C-lectin like region and regulatory motifs crucial for cell-matrix interactions (Zhang et al., 1998). The G3 domain of versican may also play a role in cell proliferation due to EGF-like motifs included in the domain (Fig. 7) (Zhang 1998). Due to alternative splicing versican has four different isoforms: V0, V1, V2, and V3. The V0 isoform, has all four functional domains and V3 has only the G1 and G3 domains. Both the V1 and V2 isoforms contain G1 and G3 domains, but V1 has only the GAGβ domain and V2 only GAGα (Shinomura et al., 1993).

Figure 2. Diagram of the 4 isoforms of Versican.

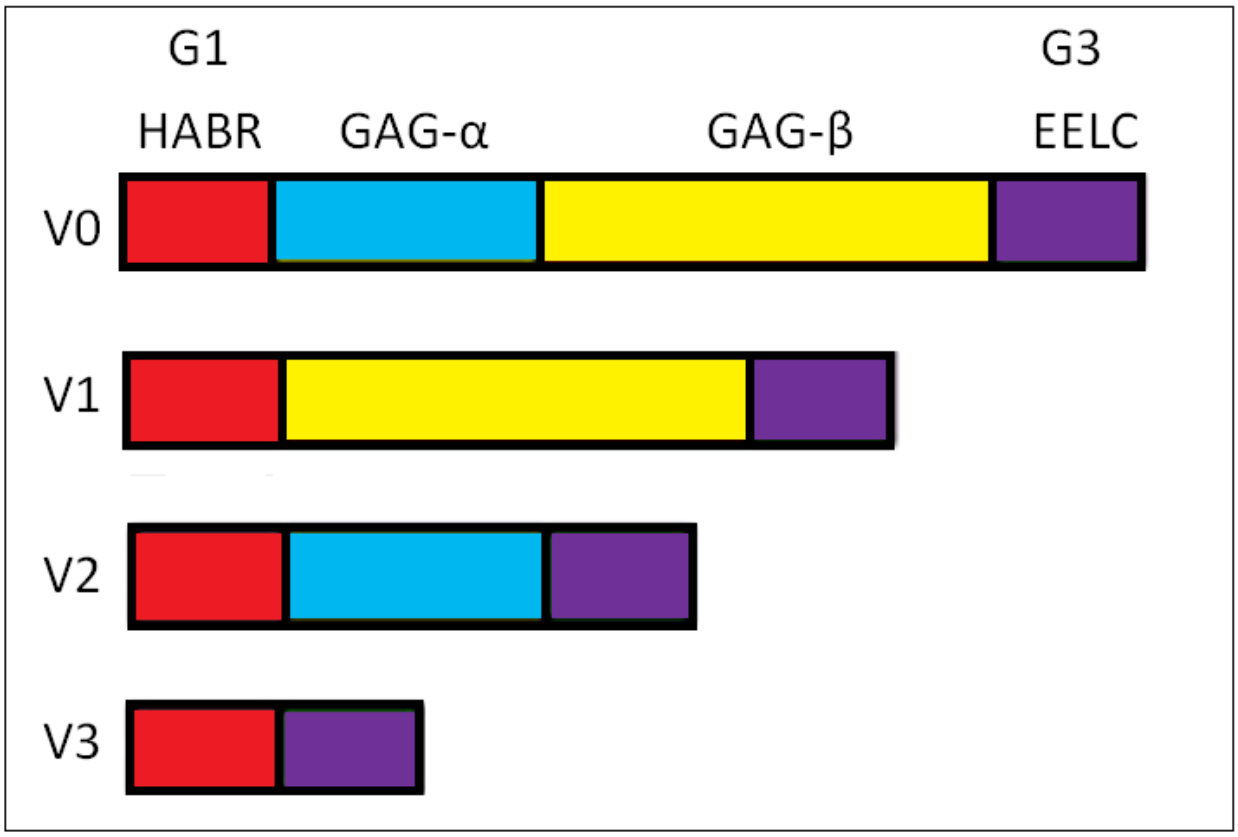

Figure 2. Diagram depicting the four isoforms of versican. The G1 functional domain is in red and contains the hyaluronan binding domain (HABR). The G3 domain is in purple and contains two epidermal growth factor repeats (EE), a lectin binding domain (L) and a complement regulatory region (C). The GAG-α and GAG-β domains are in blue and yellow, respectively. Modified from Wight 2002.

Versican's G1 domain is the hyaluronan binding domain for the chondroitin sulfate proteoglycan (Kimata et al., 1986; Zimmerman et al., 1989). Hyaluronan binds to CD44, a cell surface glycoprotein that is a primary receptor for hyaluronic acid (Rousche and Knudson 2002). It has been demonstrated that the interaction between hyaluronan and CD44 mediates cellular migration and adhesion (Lesley et al., 1993). At this time it is not known whether G1 versican modulates hyaluronan-CD44 interaction.

Previous studies have shown that ADAMTS family members, matrix metalloproteinases, have the ability to regulate versican activity through proteolytic cleavage (Capehart 2010, Sandy et al., 2001; Russell et al., 2003; Kern et al., 2006). DPEAAE is the terminal neoepitope sequence generated when the V1 isoform of versican is cleaved by ADAMTS-1, -4 or -5 (Sandy et al., 2001; Longpre et al., 2009).

The DPEAAE neoepitope is immunolocalized with full length versican, hyaluronan, link protein, and ADAMTS-1 in the murine joint interzone (Capehart 2010). This localization leads to the question as to the significance of this proteolyzed versican during joint morphogenesis. Because versican cleavage by ADAMTS generates a versican fragment containing the hyaluronan-binding G1 domain (Sandy et al., 2001), it is possible that this G1 fragment is able to function in the ECM during joint morphogenesis independent of the intact proteoglycan.

Figure 3. DPEAAE fragment in V0 and V1 isoforms of versican.

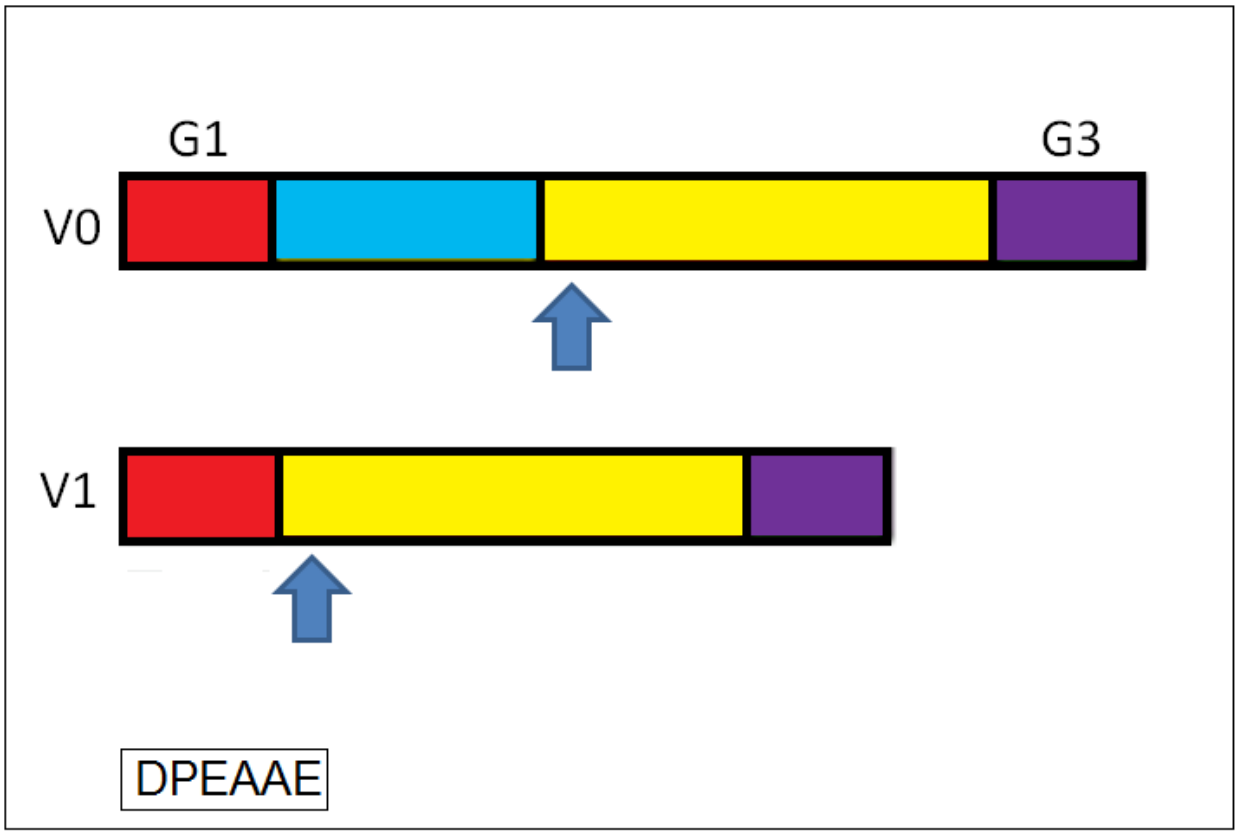

Figure 3. Schematic showing the location of the DPEAAE neoepitope created by the cleavage of the V0 and V1 isoforms if versican by ADAMTS-1 (Modified from Sandy et al., 2001).

A previous study has shown that individual versican domains could function separately during establishment of cartilages in early limb skeletogenesis as seen by enlargement of skeletal primordia due to adenoviral-mediated over expression of G1-versican (Hudson et al., 2010). Moreover, versican reduction through use of adenovirally encoded shRNAs results in diminution of joint interzone area due to alterations in organization of interzone cells, as well as reduction of other ECM components including hyaluronan, collagen II, link protein 1, and tenascin (Nagchowdhuri et al., 2012).

The present study was undertaken to validate previous RNA microarray data compiled from four arrays that manipulated versican expression in developing joint tissues. Arrays tested two different groups of pooled RNA: one in which the G1 domain of versican was overexpressed and the other in which combinatorial versican shRNA knockdown was achieved by targeting the mRNA at nucleotides 320-338 and 5334-5352 (Nagchowdhuri et al., 2012). Total RNA was sent to the Genomics Core at University of North Carolina at Chapel Hill for performance of the microarray experiment. An extensive list of genes was compiled whose expression was altered relative to wing samples receiving control adenovirus treatment. Genes that showed potential relevance to joint morphogenesis were compiled into a candidate gene list to be further validated (Table 1). That candidate list was then consolidated to focus on transcripts involved in the hyaluronan and Wnt/PCP pathways in response to G1 versican over-expression. These two pathways are of importance to this study because of their potential involvement in joint development. Synthesis and accumulation of hyaluronan leads to separation of tissues in the interzone, which begins the cavitation process leading to synovial joint formation (Pacifici et al., 2005). As the Wnt/PCP pathway is involved in cellular movement and orientation (Komiya et al., 2008, Li and Dudley, 2009), this non-canonical mechanism could affect the cavitation

process and joint development. The present study used RT-PCR and qRT-PCR to validate the fold changes calculated by the microarray analysis.

Table 1. Fold change (+/-) mRNAs in response to adneo-G1 versican over-expression and versican knockdown in HH35 (e9) (Hamburger and Hamilton, 1951) chick elbow region.

Gene Name	Accession Number	Fold Change
Hyaluronan Pathway Related Genes		
Hyaluronidase 2	XM_414258	+2.5
Hyaluronan synthase 3	XM_425137	+2.5
UDP Glucose dehydrogenase	NM_001012581	-1.9
Link Protein 1	NM_205482	-1.7
KIAA0527 protein	XM_418822	+2.4
Wnt Pathway Related Genes		
Wnt4	NM_204783	+2.4
Frizzled 2	NM_204222	+2.4
Frizzled 7	NM_204221	+2.2
Frizzled 8	XM_426568	+2.5
Frizzled 9	AF224319	+2.0
Vang-like protein 2	XM_424509	+1.8
Dachsous 1 (pcdh 16)	XM_417264	+2.2
Abl 1 tyrosine kinase	XM_422269	+2.2
Other Genes Related to Limb/Joint Development		
Noggin	BU394215	+2.8
N-WASP	TC224195	+2.2
Sox4	TC201014	+2.9
Gene Affected by Versican Knockdown		
Mastermind1	XM_414606	-1.9

SUMMARY OF CANDIDATE GENES (Table 1)

HYAL2 – Hyaluronidase 2 (Hyal2) hydrolyzes hyaluronan of high molecular mass into intermediate size fragments, about 20 kDa in size (Lepperdinger 2001). It has been debated where these hydrolysis reactions occur because Hyal2 has a pH-optimum at approximately 4, which suggests that it is a lysosomal enzyme (Lepperdinger 2001). But, recently it has been shown that the Hyal2 protein could be a GPI-anchored cell surface protein in frog oocytes when the Hyal2 mRNA is injected (Lepperdinger 2001). Hyal2 has also been found as a GPI anchored cell-surface protein in humans (Rai SK 2001). The breakdown of hyaluronan by HYAL2 could lead to the disorganization of the ECM, so that cells are able to move apart during cavitation. Hyal2 was found to have a +2.5 fold change when the G1 domain of versican was upregulated (Table 1).

HAS-3 – Hyaluronan synthase 3 (HAS-3) produces linear polymers of hyaluronan (HA) of smaller molecular sizes than those produced by HAS-1 and HAS-2 (David-Raoudi 2009). Despite the multifunctional role of HA in joints, little is known about the mechanisms that govern the activity of the HAS molecules and their relative contribution to the HA polymers produced by synoviocytes (David-Raoudi 2009). HAS-3 was found to have a +2.5 fold change when the G1 domain of versican was upregulated (Table 1), raising the possibility that shorter length hyaluronan chains are important during the cavitation process.

UDP Glucose Dehydrogenase – The enzyme UDP-glucose dehydrogenase converts UDP-glucose to UDP-glucuronate, a critical component of the glycosaminoglycans, hyaluronan, chondroitin sulfate, and heparan sulfate (Spicer 1998).. UDP-glucuronate provides the D-

glucuronate of HA, chondroitin sulfate, and heparan sulfate and, through C5 epimerization, the iduronate of HS and dermatan sulfate (Kornfeld, 1980). UDP-glucose dehydrogenase had a fold change of -1.9 (Table 1), which suggests that production of hyaluronan may be slowed, possibly playing a role in destabilization of the ECM prior to cavitation.

Link Protein 1 - Hyaluronan and proteoglycan link protein 1 is known to interact with the G1 domain of versican (Matsumoto 2003). The interaction between link protein 1, hyaluronan, and the G1 domain of versican helps to stabilize cartilage formation in the developing joints of humans (Seyfried 2005). Link Protein 1 had a fold change of -1.7 (Table 1), suggesting that down regulation could act to de-stabilize the versican/hyaluronan interaction during joint development.

KIAA0527 protein – Little is known regarding KIAA0527, also known as sushi domain-containing protein (SUSD5); however, it has been shown that KIAA0527 does contain putative hyaluronic acid–binding domains (Vincent 2008). It is shown in Table 1 that KIAA0527 had a fold change of +2.4, raising the possibility that an alternative hyaluronan receptor may be expressed in joint-forming tissues during the cavitation event.

WNT4 – Wnt signaling controls a number of processes during limb development including initiating outgrowth and control of patterning (Loganathan 2005). Wnt 4 expression was reported to be first visible at HH 27 (e5) in the developing elbow joint and from HH30 (e7) onward in the joint regions of the digits (Kawakami et al. 1999); however, recently Wnt 4 expression has been detected in the central elbow region and joint interzones of the wrist-forming region as early as

HH 26 (e5.5) (Loganathan 2005). It has also been shown that during later stages Wnt4 expression localizes in joint-forming regions throughout the limb (Loganathan 2005). Expression of Wnt 4 suggests that it is a possible candidate involved in the joint-induction process (Hartmann and Tabin 2001). Wnt4 is expressed at HH28 (e6) in the interzone and mesenchyme surrounding joints (Church et al., 2002). Wnt4 is expressed in regions of hyaluronan synthesis suggesting that Wnt4 may be a regulator of hyaluronan production. High levels of hyaluronan prevent chondrogenesis by inhibiting the early steps of cell aggregation, and hyaluronan is also a key component of joint cavitation (Toole, 1981; Dowthwaite et al., 1998). It has been reported that Wnt4 is also involved in non-canonical Wnt signaling and that overexpression of *Wnt-4* accelerates chondrocyte differentiation, (Bergenstock 2007). Table 1 shows that Wnt4 has a fold change of +2.1 in tissues over-expressing the versican G1 domain.

Frizzled 2,7,8,9 – The Frizzled family of genes codes for 7-transmembrane proteins that are receptors for the Wnt signaling proteins. It has been shown that interaction of Wnt with its Frizzled receptor triggers three different types of pathways: Wnt/Bcatenin pathway (canonical pathway), the Wnt/Ca^{2+} pathway and the Wnt/PCP (Davis 2008). It has been shown in *Xenopus* that overexpression of Frizzled 7 activates a non-canonical Wnt pathway leading to the recruitment of protein kinase C (PKC) to the membrane (Medina 1999). In *Xenopus* Frizzled 8 interacts with Wnt 5a in the non-canonical pathway (Wallingford 2001) and in rat Wnt 5a and Frizzled 2 interact to activate non-canonical, β-catenin independent, Wnt-signaling pathway (Jiang 2006). It has been shown that Frizzled 9 may play a role in the canonical and non-canonical Wnt signaling pathways in the mouse hippocampus (Zhao 2005). Little is known of these Frizzled genes and their interaction with their Wnt ligands in developing chick embryos.

Frizzled 2 had a fold change of +2.4, Frizzled 7 had a fold change of +2.2, Frizzled 8 had a fold change of +2.5, Frizzled 9 had a fold change of +2.0 in tissues over-expressing the versican G1 domain (Table 1) Because Frizzleds play a role in the non-canonical/PCP pathway this upregulation could lead to changes in organization of the actin cytoskeleton, which could potentially affect cell structure and movement in the developing joint.

Strabismus/Van Gogh-like protein 2 (Vangl2) – It has been shown in *Drosophila, Xenopus,* and zebrafish that Vangl2 functions in the planar cell-polarity pathway (Park 2001). Vangl2 actually antagonizes the canonical Wnt/β catenin pathway in zebrafish and promotes activation of c-Jun/NH2-terminal kinase (JNK) by activating c-Jun-transcription factors, such as AP-1 (Park 2001). Vangl2 had a +1.8 fold change in tissues over-expressing the versican G1 domain (Table 1). Vangl2 has also been seen in gain- and lose-of-function experiments to play a role in cell orientation in proliferative growth plate chondrocytes (Li and Dudley, 2009).

Dachsous – Dachsous is a member of the cadherin family, which encodes calcium dependent cell-cell adhesion molecules of the protocadherin family. Little is known of Dachsous interactions in chick, but Dachsous has been seen in *Drosophila* to play a role in the planar cell polarity pathway to modulate frizzled activity (Fanto 2004). Dachsous was seen to have a fold change of +2.2 in tissues over-expressing the versican G1 domain (Table 1).

Abl1 tyrosine kinase – The Abl1 protein is a non-receptor tyrosine kinase involved in many facets of mammalian development (Li, 2000). In humans ABL1 is active in processes such as cell differentiation, division, adhesion, and stress response (Shaul, 2005). In mice, ABL1 is also

widely expressed, but most notably high levels of ABL1 are found in hyaline cartilage in the adult, bone tissue in newborns, and osteoblasts and associated neovasculature at sites of endochondral ossification in the fetus (Li, 2000). Abl1 tyrosine kinase was seen to have a fold change of +2.2 in tissues over-expressing the versican G1 domain (Table 1). Abl1 tyrosine kinase has also been seen to play a role in actin cytoskeleton organization in the PCP/Pathway (Li, 2000).

Noggin – Noggin is a protein that plays a crucial role in bone development, joint formation, and neural tube formation in mice (Guo, 2004). It has also been seen that Noggin impacts the Wnt pathway by interacting with Wnt9a, Wnt16, and Wnt4, all of which have been shown to be involved in the non-canonical Wnt pathway. Noggin is required for chondrocytes to respond to joint inducing signaling; a new joint only forms in a distance where active Noggin protein concentration recovers from inhibitory signals sent by Wnts, Gdf5, and Bmps from the previously formed interzone (Guo, 2004). Noggin was seen to have a fold change of +2.8 in tissues over-expressing the versican G1 domain (Table 2).

SOX4 - SRY-related HMG box *(Sox)* genes encode a family of transcription factors crucial for embryonic development. Thirty different members of the SOX family have been found and are expressed in many different cell types at multiple stages of development (Wegner 1999). Sox4 appears critical for normal development and B-cell maturation; however, its function(s) in these processes is not yet clear. Recent studies have demonstrated high expression of Sox4 in several tumors including breast cancer, colon cancer, salivary adenoid cystic carcinoma, and medulloblastomas, suggesting that Sox4 may play a role in tumorigenesis (Frierson 2002). Sox4

enhances the Wnt signaling pathway (Sinner 2007) increasing ß-catenin stability (Lee 2010). SOX4 was seen to have a fold change of +2.9 in tissues over-expressing the versican G1 domain (Table 2).

Mastermind1 – Mastermind-like 1 (Maml1) is an important part of the Notch pathway whose function is still poorly understood. Maml1 encodes a nuclear coactivator protein that binds to the ankyrin repeat domain of Notch proteins; it forms a trimeric complex with the intracellular domain of Notch and the DNA binding protein, CSL (CBF1, Suppressor of Hairless, Lag-1) (Jefferies 2002). The Notch pathway could be necessary for processes involved in joint cavitation such as, cell proliferation and differentiation and the formation of cell boundaries (Williams et al., 2009). It has also been reported that Maml1 acts as a specific coactivator of β-catenin/TCF and plays a critical part in the Wnt pathway essential in β-catenin mediated tumorigenesis (Alves-Guerra 2007). Maml1 was seen to have a fold change of -1.9 in tissues where versican levels were reduced (Table 3).

2. Methods

Presumptive elbow joints of the developing chick limb were microinjected at stage 25 (HH25, e5) with 1-1.5 x 10^6 ifu (infectious units) of adenoviruses encoding versican shRNAs (Nagchowdhuri et al., 2012) or G1-domain Hudson et al., 2010) and viral controls using microcapillary pipets linked to a pneumatic pump (PV820, World Precision Instruments). Once injected, the eggs were returned to the incubator until stage HH35 (e9). At HH35 embryos were removed, elbow regions dissected and RNA extracted (RiboPure Kit, Ambion). The RNA concentration was determined (Nano Drop Spectrophotometer ND-1000). Each extracted RNA yielded a 260/280 ratio of 2.11 and a concentration of 249.0 ng/μL in the G1-domain RNA and 260/280 ratio of 2.09 and concentration of 214.1 ng/μL in the versican knockdown RNA.

Complementary DNA (cDNA) samples were reverse transcribed using a SuperScript III First Strand Synthesis Kit (Invitrogen). There were three different pools of RNA: a versican knockdown RNA that had two biological replicates; an overexpressed G1-domain RNA that had five biological replicates (two biological replicates from one set of injections and three biological replicates from another set of injections); and an untreated control RNA that had five biological replicates. All of these RNA samples were reverse transcribed with equal amounts of RNA (750 ng/reaction) using oligodT priming. Once RNA was reverse transcribed into cDNA, samples were diluted 5 fold for reverse transcription PCR (RT-PCR).

Primers for candidate genes were designed using the BLAST function on the NCBI website (http://blast.ncbi.nlm.nih.gov/). Forward and reverse primers were designed and the predicted amplicon sequence was searched against the chick genome to ensure that the amplicon was sequence specific. Once primers were designed they were tested using PCR to ensure that the expected amplicon could be amplified in each cDNA pool.

RT-PCR reactions were carried out in 25 µL volumes with 2.5 µL Buffer, 0.75 µL $MgCl_2$, 0.5 dNTPs, 0.125µL Taq Polymerase, 1.0 µL template cDNA, and 2.5 µL of forward and reverse primer (0.3 mM). RT-PCR was carried out in a thermocycler **(**Eppendorf Mastercycler Gradient**)** for 35 cycles with an initial denaturation step at 94°C for 2:00 min, a second denaturation at 94°C for 0:30 sec, an annealing step at the optimal annealing temperature for the specific primer pairs for 0:30 sec, an elongation step at 72°C for 0:30 sec. Once all the cycles were complete there was a final elongation step at 72°C for 10:00 min and then the machine would hold the finished PCR product at 15°C until removal for analysis.

Products were analyzed by agarose gel electrophoresis on 1.5% gels. Gels were made with 50mL of 1X TAE Buffer and 0.75g of agarose. Once completed dissolved and cooled 5µL of ethidium bromide was added and poured into the electrophoresis tray. Gels polymerized for a minimum of 45 minutes before diluted PCR products were loaded into the wells. PCR products were diluted 1:4 with loading dye (Blue Juice, Invitrogen). Gels were run using approximately 85V over one hour, and then viewed under ultraviolent light to observe PCR products. The primer pairs that were successful in this procedure are listed in Table 2. Some gene candidates were removed from further investigation after this point because successful primers were unable to be made, following multiple attempts.

Primer pairs successful for RT-PCR were then used in real-time PCR experiments to determine levels of candidate gene expression in the RNA populations extracted from versican adeno-shRNA and -G1 infected limbs relative to viral control injections. RT^2 SYBR Green/ROX qPCR Master Mix (SA Biosciences) was used for real-time PCR, this mixture is specifically used for the qPCR machine (ABI 7300). The real-time reactions were carried out in 25µL volumes containing 1.0µL of cDNA, 12.5µL of RT^2 SYBR Green/ROX qPCR Master Mix (SA

Biosciences), 0.5µL of both the forward and reverse primer. The recommended real-time thermal cycler program provided by SA Biosciences was followed, which consisted of a 10 minute initial denaturation at 95°C, then 45 cycles of 95°C for 15 seconds, 60°C for 60 seconds. β-actin primers (F: CACAGATCATGTTTGAGACCTT, R: CATCACAATACCAGTGGTACG; Accession # L08165; DeBoever et al., 2008) and GAPDH (F: GGCACGCCATCACTATC, R: CCTGCATCTGCCCATTT; Accession # K01458.1; DeBoever et al., 2008) were used as housekeeping genes.

Fold change was calculated using the Pfaffl method (2001) for relative quantification calculations by normalizing the C_T values with the house keeping genes to obtain a ΔC_T. ΔC_T was then analyzed relative to untreated control ΔC_T to obtain $\Delta\Delta C_T$. The equation $2^{-\Delta\Delta C}{}_T$ was used to calculate fold change (Pfaffl, 2001). Efficiency was also calculated using the formula $E = (10^{-1/slope}) - 1$ (Higuchi et al., 1993). The slope was calculated from standard curves generated by plotting the C_T vs. the log of the dilution of template. Statistical significance was also calculated using the Student *t*-test.

3. Results

To validate the previously obtained microarray data another form of quantifiable expression needed to be shown. Real-time PCR is becoming a more widely used technique to quantify expression (Nolan et al., 2006). Other steps had to take place before the real-time PCR could be undertaken, including primer design and RT-PCR. Primer design was of the utmost importance because amplicons needed to be sequence specific to that particular gene. RT-PCR verified that products of the predicted size could be amplified from the template cDNA. RT-PCR demonstrating presence of transcripts, but could not quantify the level of expression. Through a series of calculations real-time PCR could yield quantifiable fold change expressions levels that could validate the microarray data.

RT-PCR

Primers were designed for all genes in the candidate list (Table 1) and tested using RT-PCR. Primer pairs shown in Table 2 were working primer pairs used for further analysis. Genes for which successful primer pairs could not be obtained were Frizzled 8, Sox4, and N-WASP. Multiple primer pairs were designed and tested before it was decided to omit further analysis of those genes. When a band was visible at the predicted length, then the PCR product was accepted as successful. Figure 4 shows bands of these PCR products; once accepted, primer pairs were used for real-time PCR.

Table 2. Genes, Accession numbers, primer pairs, and expected sequence length for candidate genes tested in RT-PCR and Real Time-PCR.

Gene Name	Accession #	F. Primer: 5'-3'	R. Primer: 5'-3'	Sequence Length
Mastermind	XM_414606	GCAGTCCAGCTCCAGCCAGC	GAACAGCAGCACCCTGGCCC	179
CABL	XM_422269	ATTGTGGGCACGGTCCTGTTCC	TGCCTGGGGTTCGACATCGC	150
Dachsous	XM_417264	GCGAGGACCCAATGGGGTGC	GGCGGGAGCGTTGTCGTTGA	175
Frizzled 2	NM_204222	TTCCGCCAGCACTGGGAGCG	CGCTCACACCGTGGTCGCGCC	245
Frizzled 7	NM_204221	CTGCTGTCAAAACCATCACC	GCACCATCAGCTTCTCCAGC	243
Frizzled 9	AF224319	CTCACCTTCCTGCTCGACCCGC	CAGAGCGAGCTGGCCATGCC	239
HYAL 2	XM_414258	GGCTGCAGGAGAACATCGG	GCGTAGCGCAGCGTTGTCAC	247
HAS3	XM_425137	GTGGACTACATCCAGGTGTG	GAAGGCCATCCAGTACCGCA	180
KIAA0527	XM_418822.2	ACCACGGGATGGCTGGCTGA	TCTCCGCACGGCTTGTCTTC	167
Link Protein	NM_205482	GACACCACAGAAAGAGCTAC	GCTGTGTCGTCCTCTAATCC	154
Noggin	NM_204123.1	CGCTTTTGGCCCCGGTACGT	GATGGGGTACTGGATGGGGA	174
Vangl2	XM_424509	GAGGACAGCGCGCACCTGGAC	CGCGCGGAAGACGAAGACGC	264
UDPGDH	NM_001012581	GACAGGGTGCTCATTGGTGG	GCTGCCTCCAAACCCAACAC	310
Wnt4	NM_204783	TCGAGCAGAGCGAGATCGGC	CCCGATGGCAGGGTTTGCAC	300

Figure 4. Agarose gels confirming PCR amplicons.

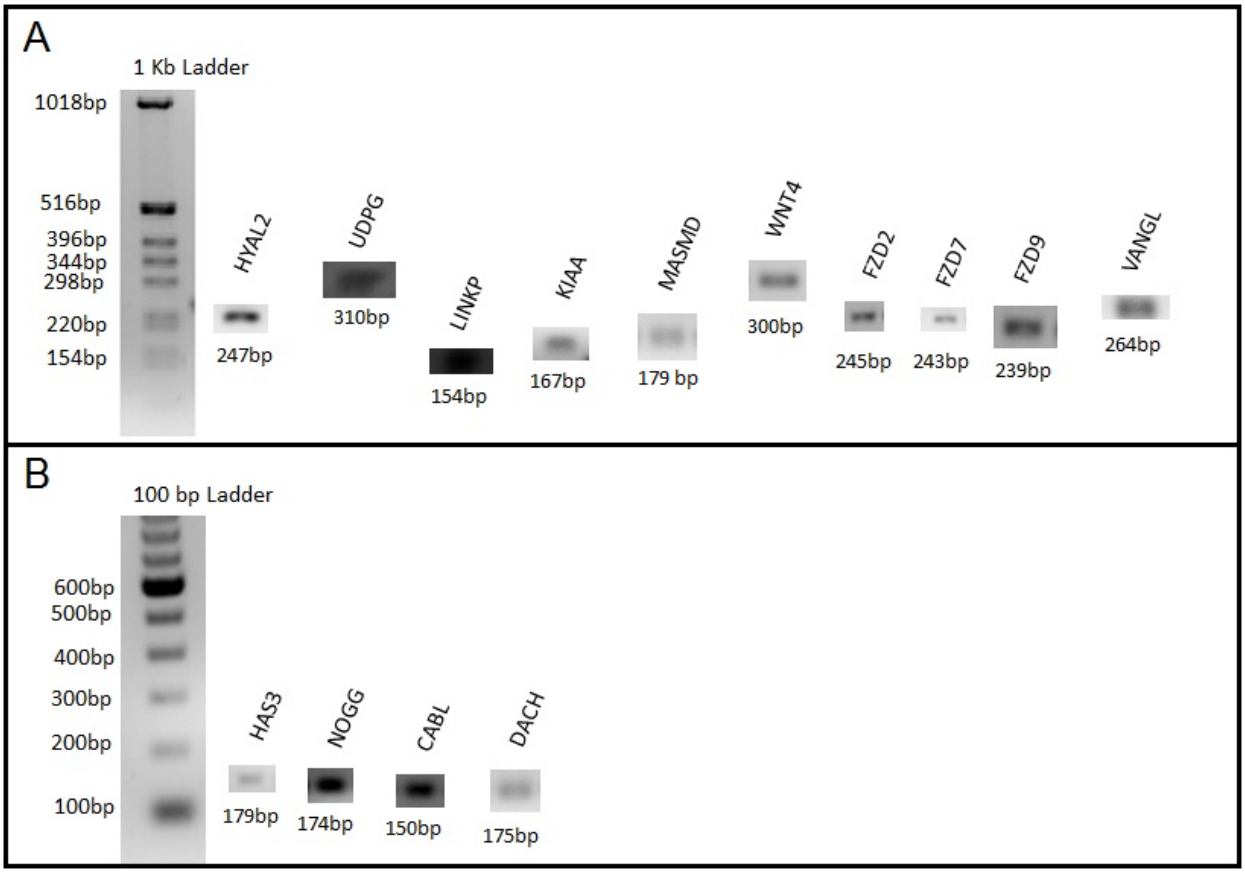

Figure 4. PCR products for genes listed in Table 2. All gels were 1.5 % agarose. A. Bands for HYAL2, UDPG, LINK, KIAA, MASMD, WNT4, FZD2, FZD7, FZD9, and VANGL with corresponding sequence sizes were compared to a 1KB standard ladder. B. Bands from for HAS3, NOG, CABL, and DACH with corresponding sequence sizes were compared to a 100 base pair ladder.

Real Time PCR

β-Actin reference gene

Real-time PCR experiments were performed to quantify levels of expression in the template cDNA. Initially, two biological replicates of both G1-domain overexpression and knock down template cDNA were used, but due to the number of genes affected by G1 versican over-expression and potential relevance to ongoing research regarding potential role of a G1 proteolytic fragment in joint development, subsequent experiments involved only samples in which the G1 domain was over expressed. These latter injections yielded three additional pooled biological replicates of G1 and control RNA that was reverse transcribed into cDNA and used for additional real-time PCR testing.

A total of five biological replicates of G1 overexpressed template cDNA were used to quantify expression levels (Fig. 5). These fold changes were tabulated over a range of 3-10 experiments and each gene of interest had at least ten technical replicates (Fig. 5). With the exception of FZD2, which was down regulated, fold changes were noted in the direction expected from earlier microarray data.

The average fold changes were calculated with primer efficiency calculated in using the formula: $E = (10^{-1/slope}) - 1$ (Higuchi et al., 1993) (Fig 6). Some genes from Figure 5 do not appear in Fig 6 due to their primer efficiency being outside the acceptable range of ~80-120% (Table 3) (HAS3, WNT4, VANGL, and CABL). Dissociation curves were analyzed to verify these primer deficiencies (Fig. 7). The dissociation curves for HAS3, WNT4, VANGL, and CABL were unacceptable because of the multiple peaks that formed during dissociation. The dissociation curve for GAPDH is shown as a reference of what an acceptable dissociation curve, uniform peaks at one temperature.

Appendix B shows averaged fold changes of the genes of interest when versican level was knocked down. These fold changes were also tabulated over five experiments and each gene of interest had at least ten technical replicates. These experiments were conducted using the initial two biological replicate pools. MASMD which had been noticeably affected by versican being knocked down showed a similar trend of down-regulation.

Figure 5. Fold Change results from initial real-time PCR experiment when G1 domain was over expressed.

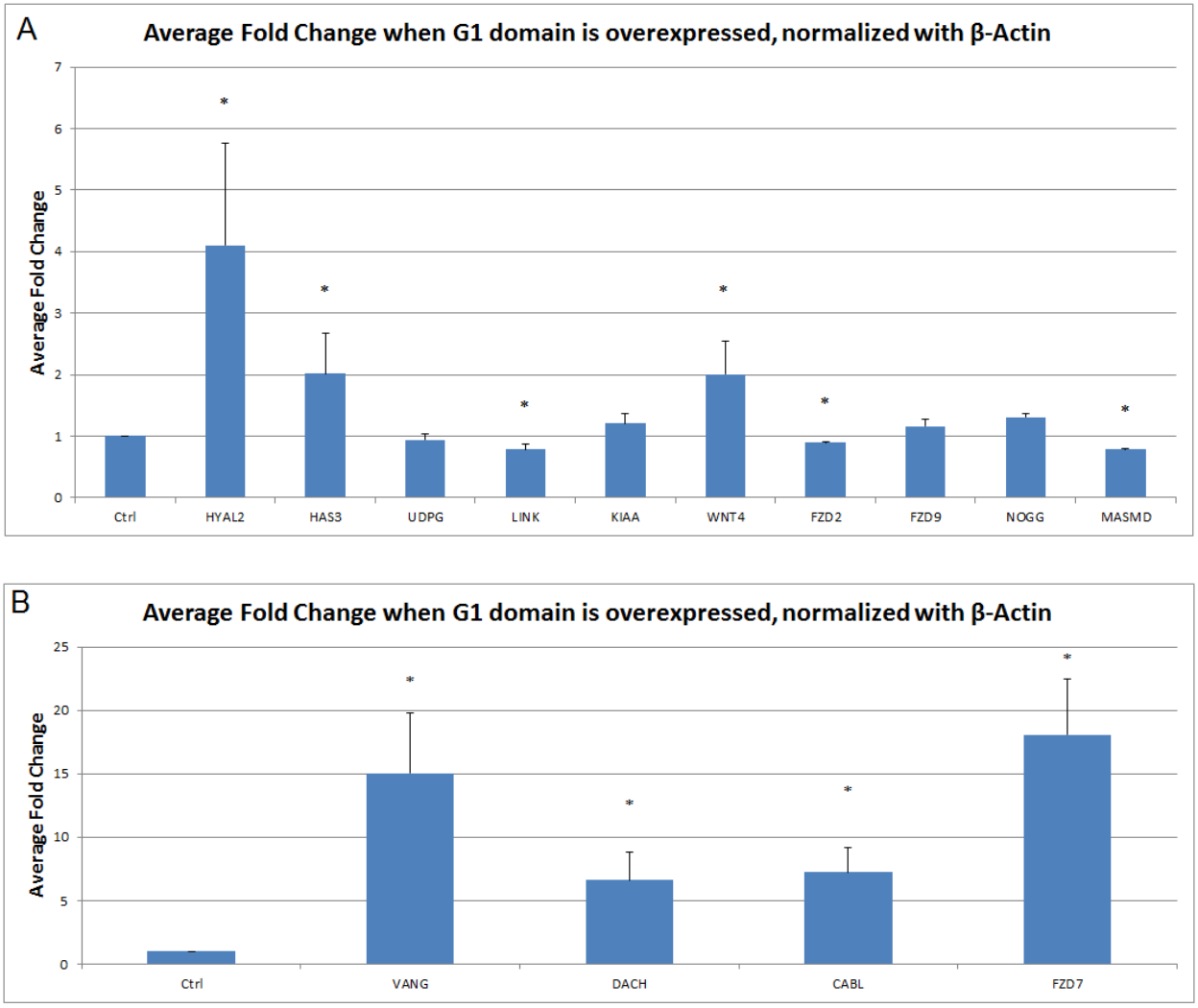

Figure 5. Average fold change from real time PCR data using template cDNA samples in which versican G1 domain was overexpressed. Panels A and B are the same treatments separated such that differences infold change can be better appreciated. Bars denote standard error of the mean and asterisks denote significance at $p < 0.05$.

Figure 6. Fold change results from G1 domain over expressed RNA.

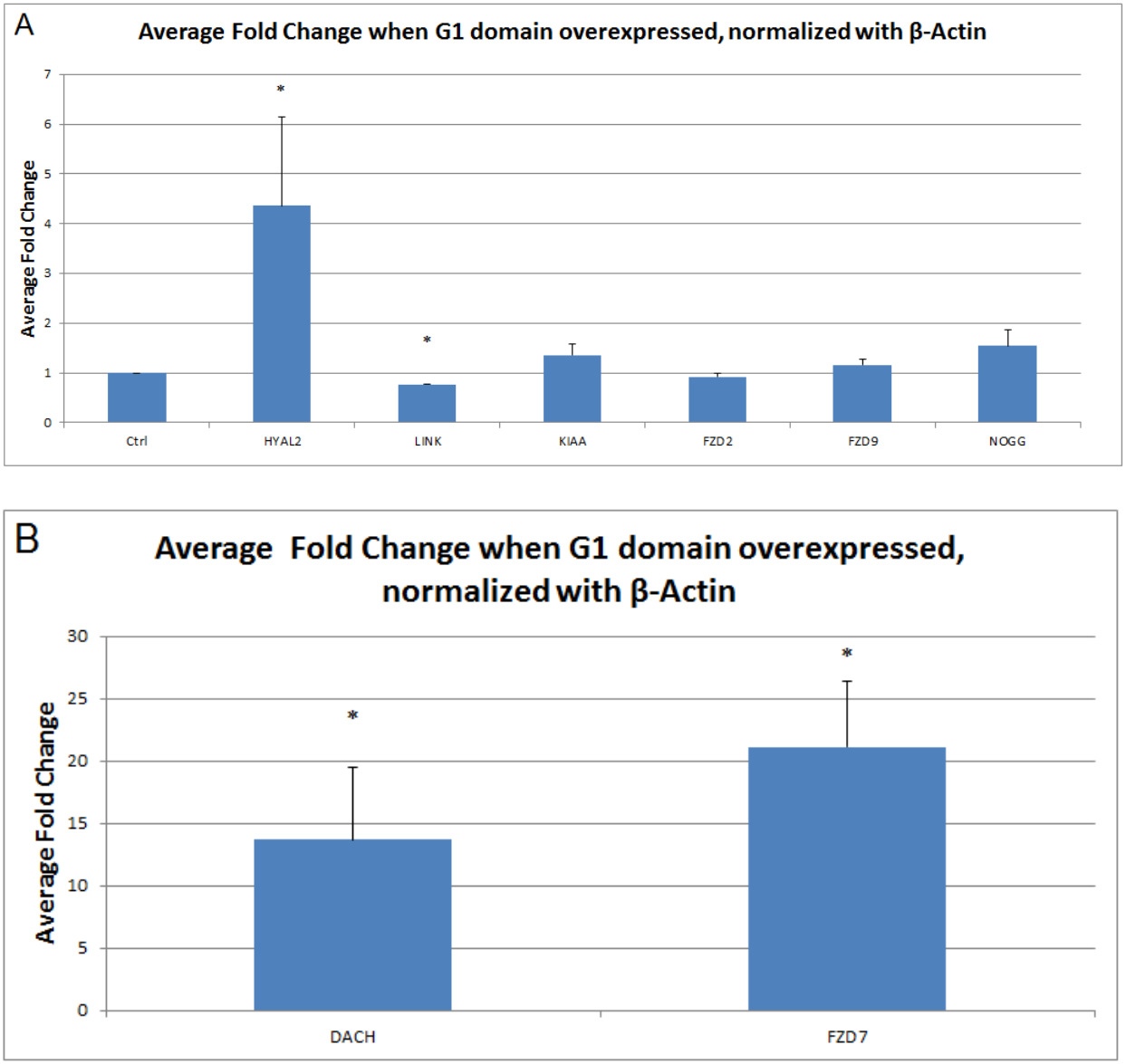

Figure 6. Average fold change from all real time PCR data using template cDNA in which versican G1 domain was overexpressed. Panels A and B are the same treatments separated such that differences infold change can be better appreciated. Bars denote standard error of the mean and asterisks denote significance at $p < 0.05$. Efficicencies (Table 3) have been calculated into these fold changes.

Table 3. Efficiency for Candidate Genes

Gene Name	Efficiency (%)
Candidate Genes	
HYAL2	102.02
DACH	124.37
KIAA	119.07
NOGG	110.28
FZD7	103.94
FZD9	98.94
LINK	81.44
FZD2	101.72
WNT4	188.34
CABL	234.98
VANGL	208.16
HAS3	322.69
Housekeeping Gene	
ACTIN	83.40
GAPDH	97.78

Table 3 shows the efficiencies that were calculated using the formula: $E = (10^{-1/slope}) - 1$ (Higuchi et al., 1993). The slope was generated from the standard curve graph.

Figure 7. Melting curves for CABL, HAS3, VANGL, WNT4, and GAPDH.

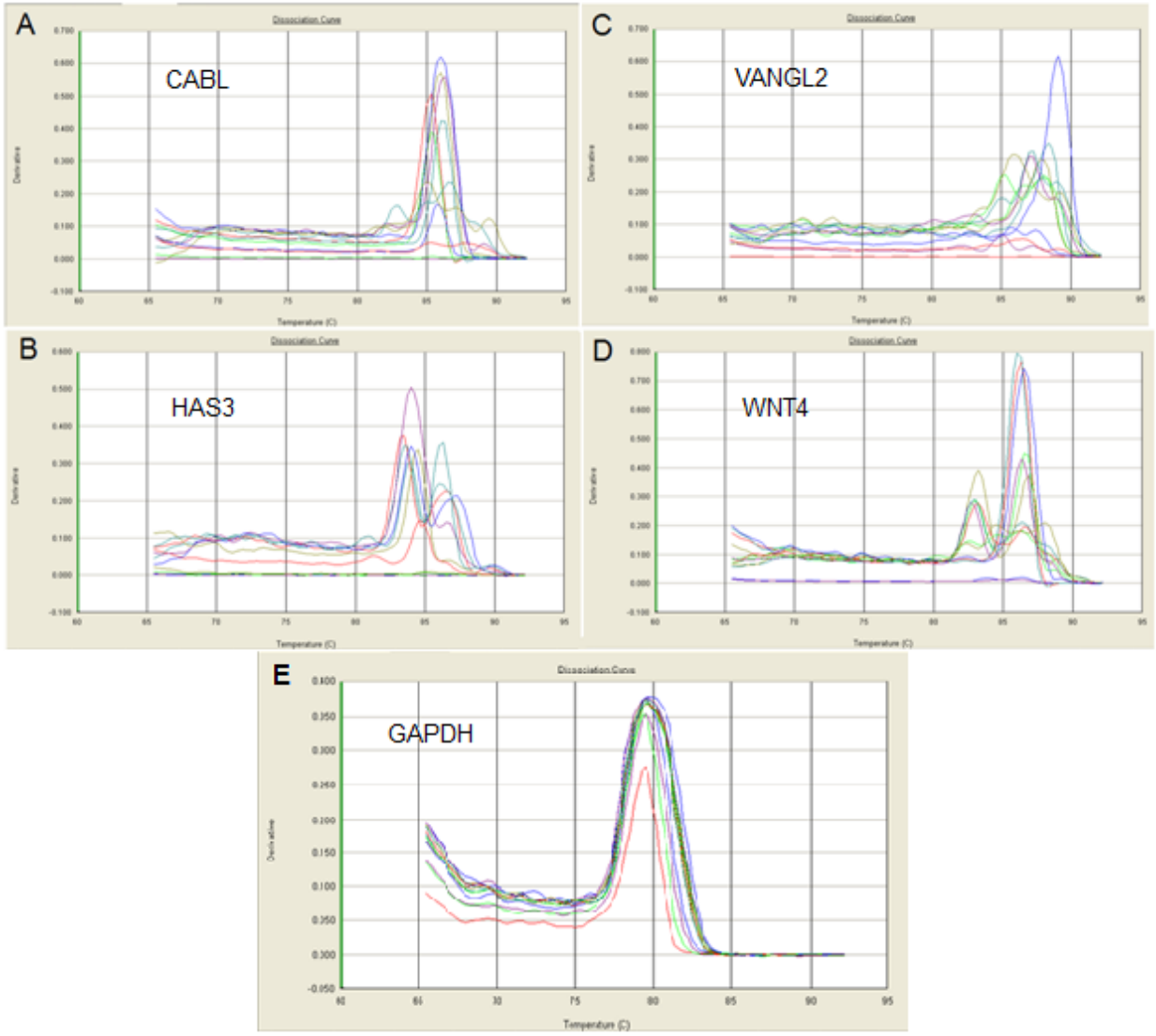

Figure 7 shows the melting curve at which the PCR products created by real-time PCR begin to denature. A. Melting curve for CABL. B. Melting curve for HAS3. C. Melting curve for VANGL. D. Melting curve for WNT4. E. Melting curve for GAPDH. Temperature is on the x-axis and the first derivative of the change in fluorescence over time is on the y-axis.

GAPDH reference gene

To ensure that the housekeeping gene, β-actin, was reliable a second housekeeping gene was used in real-time PCR experiments. Glyceraldehyde 3-phosphate dehydrogenase (GAPDH) was used as the second reference gene to strengthen the results found from experiments utilizing β-actin. Real-time PCR experiments normalized using GAPDH were performed with newly extracted RNA, so that three biological replicates could be represented in the experiments.

Versican G1-domain template cDNA was used to perform real-time PCR. C_T values from a subset of genes were normalized using GAPDH and β-Actin simultaneously and average fold changes calculated (Fig. 8). The genes included in the subset were those that had acceptable primer efficiencies (~80-120%) in Table 3. Figure 9 is a comparison between the two housekeeping genes. There were slight differences in the average fold changes when the C_T values were normalized with GAPDH, but up-regulation or down-regulation trends were similar for each candidate gene being tested.

Combined Reference Genes

Since the two reference genes were relatively similar in their respective fold change averages, the two were averaged together to achieve a more robust normalization of the data (Fig. 10). The efficiencies from Table 3 have been factored into the combined normalized fold change averages using the equation: $E = (10^{-1/slope}) - 1$ (Higuchi et al., 1993).

Figure 8. Fold change results from G1 domain over expressed RNA.

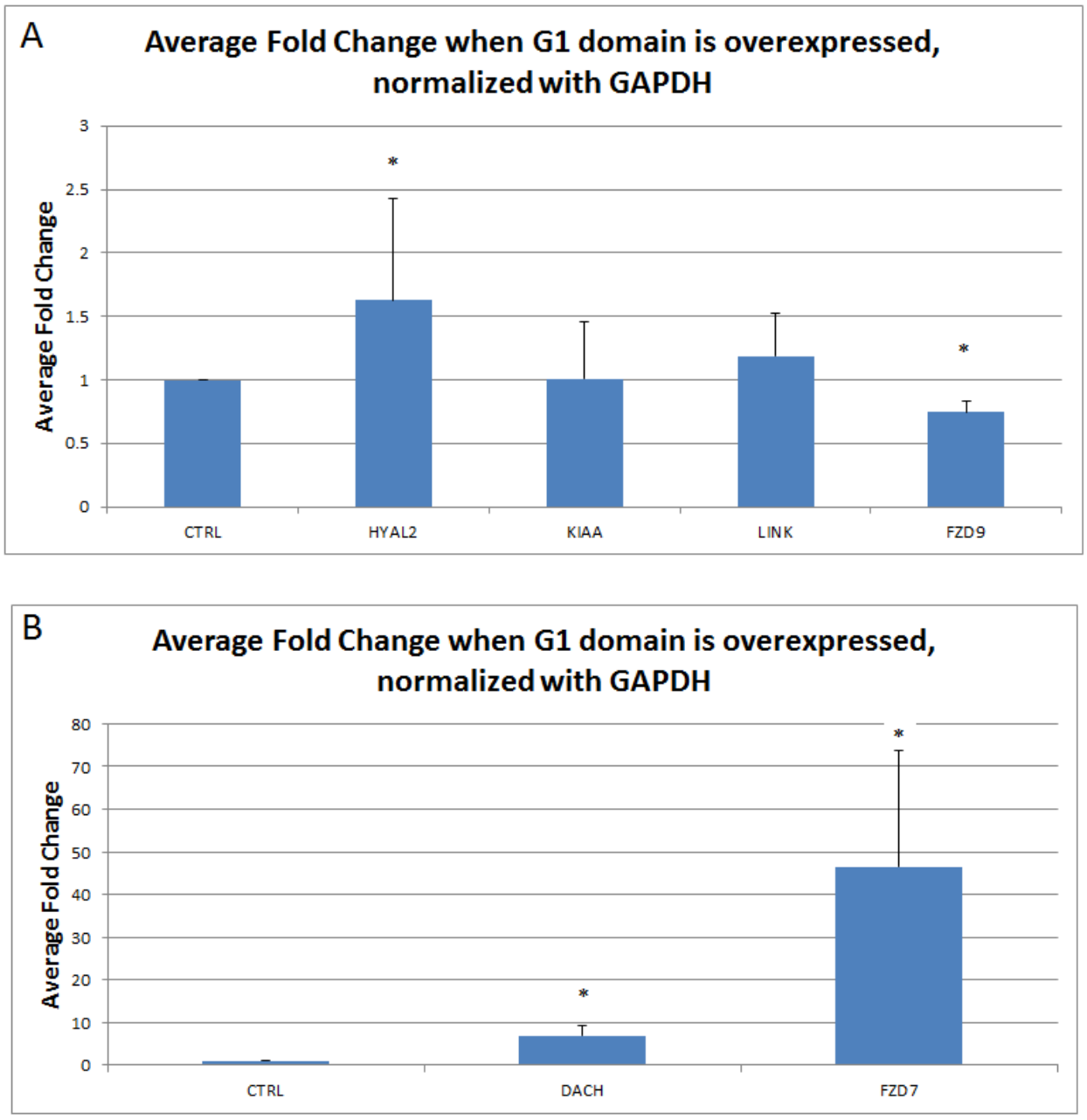

Figure 8. Calculated fold changes of real-time PCR experiments using template cDNA in which versican G1 domain was over expressed. Panels A and B are the same treatments separated such that differences infold change can be better appreciated. Bars denote standard

error of the mean and the astericks denote signifcance at $p < 0.05$. Efficiencies (Table 3) are calculated into these average fold changes.

Figure 9. Comparison between fold changes generated from the reference genes, β-actin and GAPDH.

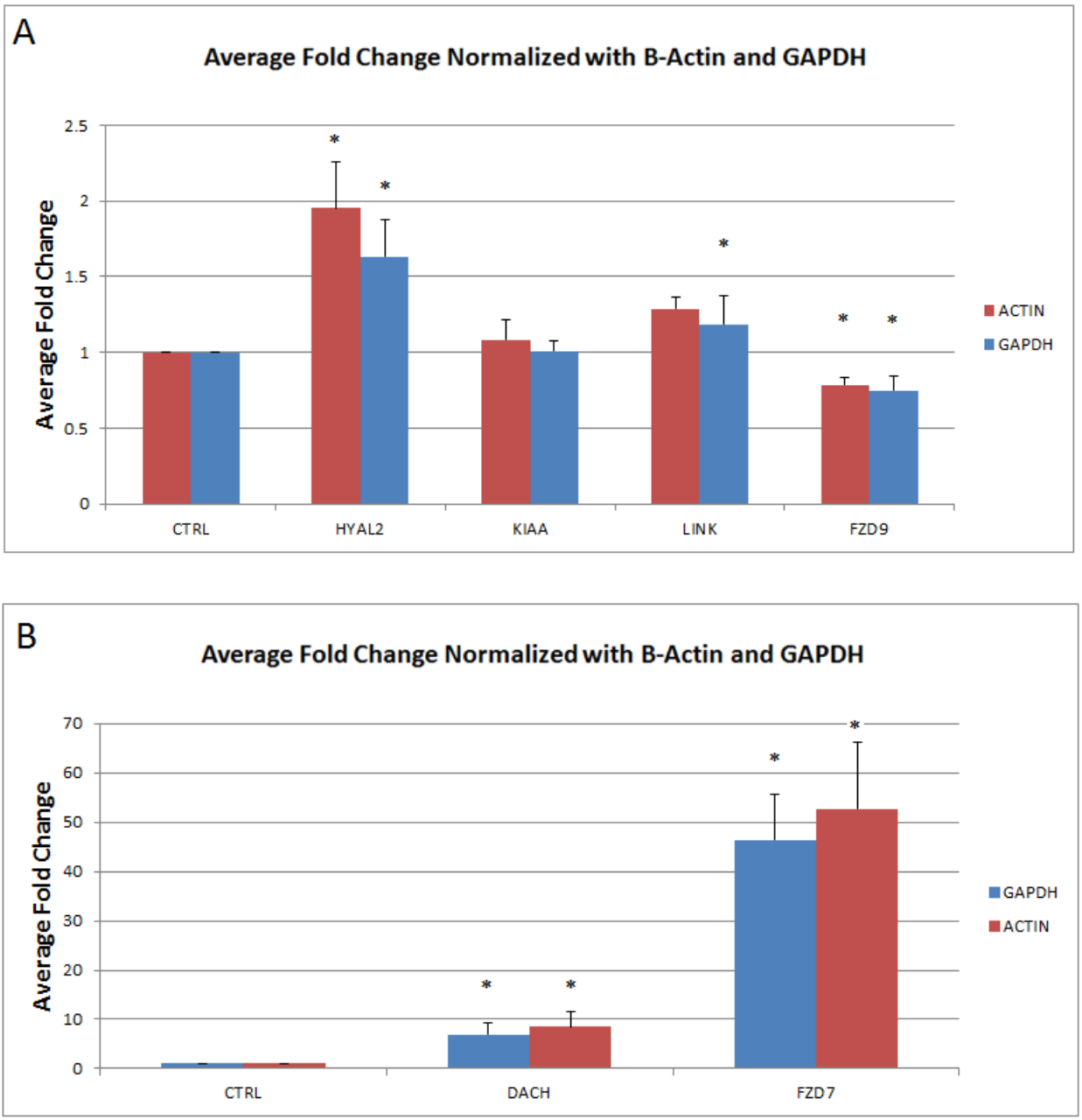

Figure 9. A subset of average fold changes to compare the two reference genes, β-Actin and GAPDH. Panels A and B are the same treatments separated such that differences infold

change can be better appreciated. Bars denote standard error of the mean and the astericks denote signifcance at $p < 0.05$. Efficiencies (Table 3) are calculated into these average fold changes.

Figure 10. Average Fold Change when G1 domain is overexpressed, normalized with both reference genes.

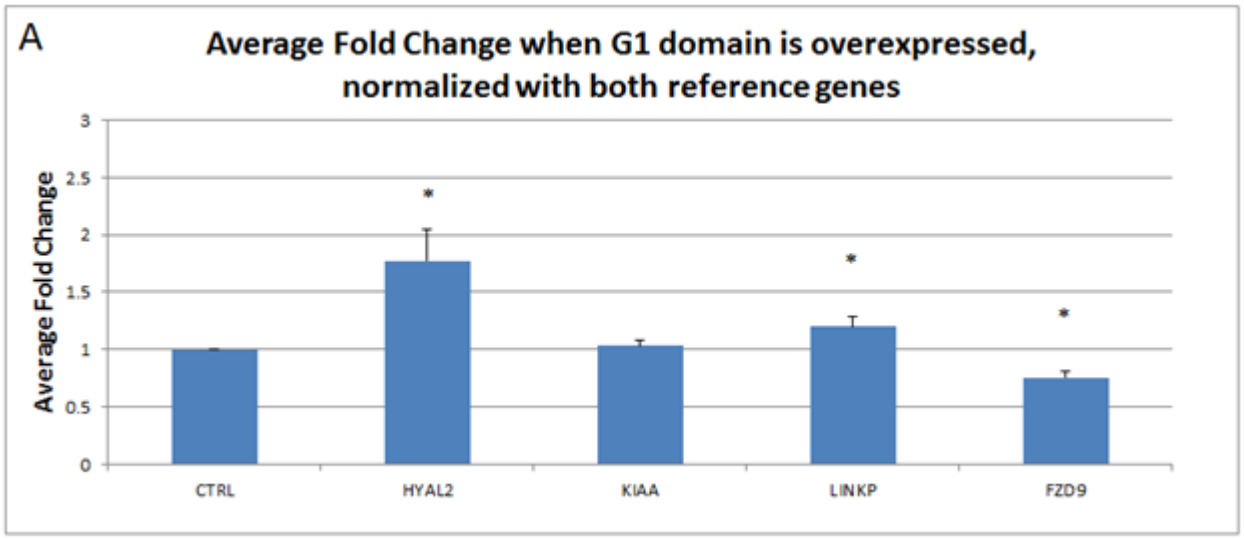

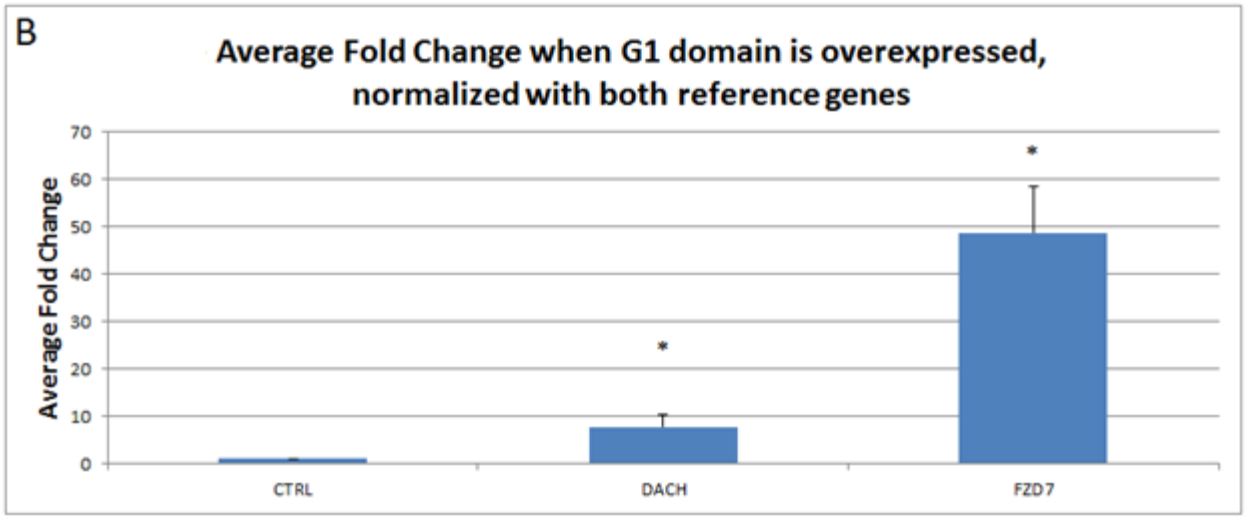

Figure 10. Calculated fold changes of real-time PCR experiments in which versican G1 domain was over expressed and normalized with a combined average of both, β-actin and GAPDH, reference genes. Panels A and B are the same treatments separated such that differences infold change can be better appreciated. Bars denote standard error of the mean and the astericks denote signifcance at $p < 0.05$. Efficiencies (Table 3) are calculated into these average fold changes

4. Discussion

Versican is a proteoglycan expressed in the interzone of the developing synovial joint in the chick limb (Shepard 2007). Versican has three modular domains: G1, G2, and G3 (Kimata et al., 1986; Zimmerman et al., 1989) and due to alternative splicing yields four different isoforms (Shinomura et al., 1993). Moreover, ADAMTS-1 cleaves V0 and V1 isoforms of versican to leave a terminal neoepitope, DPEAAE, at the carboxy end of a proteolytic fragment containg the G1 domain (Capehart 2010). This neoepitope co-localized with hyaluronan, full length versican, and link protein in the murine joint interzone (Capehart 2010). This led us to hypothesize that the G1-domain of versican may have a role in joint development and may be able to function separately from the rest of the proteoglycan.

To investigate the possibility of an independent action for G1-domain, an adenoviral construct that overexpressed the G1 domain of versican was injected into the presumptive elbow joints of chick embryos at HH25 (e5) (Hamburger and Hamilton, 1951) and used for analysis at HH35 (e9) (Hamburger and Hamilton, 1951), the stage when early joint cavitation is under way. In a separate experiment adenoviral constructs used a combination of knockdown shRNA constructs that targeted the versican mRNA at nucleotides 320-338 and 5334-5352 (Nagchowdhuri et al., 2012). The RNA from the two of injections were isolated and sent to the Genomics Core at University of North Carolina at Chapel Hill for microarray analysis. From microarray results a candidate list was formulated to investigate genes that showed potential relevance to joint morphogenesis. Genes chosen were involved in hyaluronan and Wnt pathways.

The aim of this investigation was to validate the earlier microarray data through use of RT-PCR and real-time PCR. RT-PCR was used to ensure that the primers designed for each gene were successful at amplifying the desired sequence (Fig. 4). Some gene primers were unable to

be generated: FZD8, SOX4, and N-WASP. Multiple attempts were made to design these primers before excluding them from further analysis. Primers that yielded amplicons of the predicted size from pooled samples utilized for the microarray analysis were used for real-time PCR.

Real-time PCR is a technique that amplifies a targeted DNA sequence while simultaneously quantifying the expression. The method of detection used in this study was RT^2 SYBR Green/ROX qPCR Master Mix (SA Biosciences) that binds to double stranded DNA. When the SYBR green anneals to the double stranded DNA it fluoresces and this fluorescence is detected by the PCR instrument and graphed as cycle number vs. fluorescence intensity. The C_T value is where the fluorescence crosses the threshold, which was chosen by the experimenter (1.0 was the threshold for all experiments). Once the C_T is obtained from the real-time PCR run fold change can be calculated. Fold change is calculated using the Pfaffl method (2001) for relative quantification calculations by normalizing the C_T values with housekeeping genes to obtain a ΔC_T. ΔC_T is then analyzed relative to untreated control ΔC_T to obtain $\Delta\Delta C_T$. The equation $2^{-\Delta\Delta C_T}$ is then used to calculate fold change.

Efficiency was also calculated using the formula $E = (10^{-1/slope}) - 1$ (Higuchi et al., 1993). The slope was calculated from standard curves generated by plotting the C_T vs. the log of the dilution of template. Efficiency is then used to modify the fold change calculation to obtain a more accurate fold change using the formula: $2^{-\Delta\Delta C_T * E}$.

Real-time PCR experiments were initially run with genes that had successful primer pairs from RT-PCR (Table 2). The C_T values returned from the real-time PCR experiments were normalized with the housekeeping gene, β-Actin. Using these C_T values, fold changes could be calculated (Fig 5 and 6). These experiments used five biological replicates over multiple experiments (3-10) and each experiment had three technical replicates for each biological

replicate. With the exception of a few genes, the real-time PCR data tended to agree with the microarray data. The fold changes from the two different methods of analysis were not expected to be exactly the same, but expectations were to see fold changes in the same direction.

A second housekeeping gene, GAPDH, was added to experiments to strengthen results of the study. Real-time PCR was performed with a selected subset of genes to yield C_T values and normalized with both β-Actin and GAPDH. The respective fold changes were calculated and compared (Fig 8 and 9). There were slight differences in average fold changes, but the fold changes were so similar that C_T values for the two housekeeping genes were averaged together for each cDNA pool to achieve one combined fold change for gene expression (Fig 10).

Mastermind1 was the only gene chosen for use in the present study when versican expression was reduced (App. B). As seen in Appendix B MASMD fold change was significantly reduced relative to the control. But, moving forward with experimentation this RNA was no longer used because of growing interest in the potential role of the versican G1-domain in the developing joint.

Genes with reasonable efficiency (~80-120%) were used for continued experimentation: HYAL2, KIAA, LINK, FZD9, DACH, and FZD7. Other genes were omitted either because of poor primer efficiency (CABL, VANGL2, HAS3, and WNT4) or they were less relevant to ongoing studies by this laboratory (UDPG, NOGG, and FZD2). The poor efficiencies were made clearer upon looking at the dissociation curves for CABL, VANGL2, HAS3, and WNT4 (Fig. 7). In each case there were multiple peaks denoting that multiple products were being made, either from primers not being sequence specific or the primers were self-annealing. All expected amplicon sequences were checked in the NCBI database against the *Gallus gallus* genome to

ensure sequence specificity, so unless is the primers were binding sequences not present in the database, then the likelihood is that primers were self annealing.

HYAL2 is an enzyme that hydrolyzes long, high molecular mass hyaluronan strands (Lepperdinger 2001). If HYAL2 was upregulated and expressed at the cell surface, when the G1 domain is expressed, then the joint interzone may become saturated with small molecular weight hyaluronan fragments. This could possibly be a mechanism to destabilize rigidity of the extracellular matrix.

From real-time PCR data the KIAA0527 protein was upregulated, relative to the control, by the G1-domain of versican being overexpressed. Little is known regarding this KIAA protein, its sequence suggests that is a putative hyaluronan binding protein, much like CD44 (Vincent 2008). If it is a hyaluronan binding protein it could be involved in G1-hyaluronan dynamics in this interzone pathway and act as an alternative CD44 receptor. However, the mechanisms that control KIAA0527's intracellular activities are still unknown. It would definitely be beneficial to perform in situ hybridization with KIAA to see where it is being expressed in the joint interzone, because this has not been done before.

Frizzled-9 and frizzled-7 are both involved in the non-canonical Wnt-pathway as transmembrane Wnt receptors (Zhao 2005; Medina 1999, respectively). FZD9 had fold changes that were increased compared to the control, which agrees with the microarray data. FZD7 had robust upregulation according to real-time data, which trended in the same way as the microarray result. These upregulation of FZD7 and FZD9 occur when the G1 domain of versican was overexpressed. As FZD7 works within the PCP Pathway, this pathway could be working to maintain a well ordered laminar structure among interzone mesenchyme so that when cavitation begins, cells are able to move apart in an organized fashion.

Dachsous is also upregulated in the real-time PCR data, as well (Fig. 10). This upregulation trend agrees with the microarray data from Table 1. Dachsous activity is still unknown in chick, although it has been seen to play a role in the PCP-pathway to modulate frizzled receptors in Drosophila (Fanto 2004). DACH has also been implicated in controlling the orientation of microtubules to establish planar cell polarity in the wing of *Drosophila* (Harumoto et al., 2010).

HAS3 transcript was both upregulated when the G1 domain was overexpressed before efficiency was calculated into the fold change. The large primer efficiency could be due to poor primer design or primer dimer formation during the PCR reaction. It could be due to HAS3 being a low-copy transcript (Tien and Spicer 2005), so when the cDNA becomes increasingly diluted for efficiency calculation there are only very few transcripts for the primers to bind to. As a note, it was particularly hard to design primers for HAS3. Bovine RNA was kindly provided by the Warren Knudson Lab, Brody School of Medicine, and a DNA sequence that overlapped in bovine and chick was found and tested to produce the primer pair utilized for amplification of HAS3.

The G1-domain of versican interacts with hyaluronan, which in turn may be bound to the cell surface receptor, CD44. At this time mechanisms involved in G1-domain over-expression effects on hyaluronan-CD44 interaction are unknown, but the microarray data and the real-time PCR data suggest that the G1-domain may play some role in this interaction. The G3-domain of versican binds to cell surface receptors, such as, fibronectin, fibrillin, fibulin, and collagen type I and could possibly interact with other EGF receptors (Zhang et al., 1998). The binding of the different domains of versican help to create a rigid extracellular matrix prior to cavitation.

When ADAMTS-1 cleaves the G1-domain away from the rest of the proteoglycan cell-cell interactions are disrupted and cells begin to push apart. And because of the upregulation of HYAL2 there is an abundant of small hyaluronan fragments possibly saturating the CD44 cell surface receptors. The upregulation of KIAA0527 is particularly interesting because it could be playing a role as a putative cell surface, hyaluronan binding protein, further experimentation would be needed to confirm this.

When versican is completely removed from mice limbs are noticeably shorter in length and the joints are tilted (Choocheep et al., 2010). Versican knockdown experiments show that the cells in the interzone become disorganized in the absence of versican, possibly due to effects in the PCP pathway (Nagchowhurdi 2012). The microarray data and the real-time PCR data, through upregulation of known PCP pathway components, suggest that the interaction between the G1-domain and hyaluronan could be controlling downstream events in the cell to modulate the cytoskeleton through the PCP-pathway. If the PCP pathway is regulated by G1, this could help regulate joint orientation by helping cells to align properly in the interzone prior to and during cavitation.

There is an increasing appreciation for extra cellular matrix impacts on gene expression. We have shown that when the G1 domain of version is overexpressed there are changes in gene expression, such as the upregulation of PCP pathway genes. Though the mechanisms are still unclear, the data suggests that through hyaluronan-CD44 interaction the G1 domain of versican is playing a role in intracellular gene expression. Peterson et al. (2004) showed evidence of the hyaluronan-CD44 interaction playing a role in intracellular gene expression by affecting the BMP pathway through Smad1 binding to the CD44 cytoplasmic tail. It is possible that the G1

domain could be affecting the PCP pathway genes through a similar hyaluronan-CD44 interaction, experiments to this end are pending in the laboratory.

REFERENCES

Alves-Guerra, M.-C., Ronchini, C., & Capobianco, A. J. (2007). Mastermind-like 1 Is a Specific Coactivator of β-Catenin Transcription Activation and Is Essential for Colon Carcinoma Cell Survival. *American Association for Cancer Research*, 67:8690-8698.

Bell, D. M., Leung, K. K., Wheatley, S. C., Ng, L. J., Zhou, S., Ling, K. W., . . . Cheah, K. S. (1997). SOX9 directly regulates the type-II collagen gene. *Nature*, 16:174-178.

Bergenstock, M. K., & Partridge, N. C. (2007). Parathyroid Hormone Stimulation of Noncanonical Wnt Signaling in Bone. *Annals of the New York Academy of Sciences*, 1116:354-359.

Breitschopf, H., Suchanek, G., Gould, R., Colman, D., & Lassmann, H. (1992). In situ hybridization with digoxigenin-labeled probes: sensitive and reliable detection method applied to myelinating rat brain. *Acta Neuropathologica*, 84(6):581-587.

Capehart, A. (2010). Protelytic Cleavage of Versican During Limb Joint Development. *The Anatomical Record*, 293:208-214.

Choocheep, K., Hatano, S., Takagi, H., Watanabe, H., Kimata, K., Kongtawelert, P., & Wantanabe, H. (2010). Versican Facilitates Chondrocyte Differentiation and Regulates Joint Morphogenesis. *The Journal of Biological Chemistry*, 285:27:21114-21125.

Church, V., Nohno, T., Linker, C., Marcelle, C., & Francis-West, P. (2002). Wnt regulation of choondrocyte differentiation. *Journal of Cell Science*, 115:4809-4818.

Crowe, R., Zikherman, J., & Niswander, L. (1999). Delta-1 negatively regulates the transition from prehypertrophic to hypertrophic chondrocytes during carilage formation. *Development*, 126(5):987-998.

David-Raoudi, M., Deschrevel, B., Leclercq, S., Galera, P., Boumediene, K., & Pujol, J.-P. (2009). Chondroitin Sulfate Increases Hyaluronan Production by Human Synoviocytes Through Differential Regulation of Hyaluronan Synthases. *Arthritis and Rheumatism*, 60:3:760-770.

Davis, L. A., & Nieden, N. (2008). Mesodermal fate decisions of a stem cell: the Wnt switch. *Cellular and Molecular Life Sciences*, 65:2658-2674.

Embry, J. J., & Knudson, W. (2003). G1 Domain of Aggrecan Cointernalizes with Hyaluronan via a CD44 Mediated Mechanism in Bovine Articular Chondrocytes. *Arthritis and Rheumatism*, 48(12):3431-3441.

Fanto, M., & McNeil, H. (2004). Planar polarity from flies to vertebrates. *Journal of Cell Science*, 117:527-533.

Francis-West, P. H., Abdelfattah, A., Chen, P., Allen, C., Parish, J., Ladher, R., . . . Archer, C. W. (1999). Mechanisms of GDF-5 action during skeletal development. *Development*, 126:1305-1315.

Frierson, Jr., H. F., El-Naggar, A. K., Welsh, J. B., Sapinoso, L. M., Cheng, J., Saku, T., . . . Hampton, G. M. (2002). Large scale molecular analysis identifies with altered expression in alivary cystic carcinoma. *American Journal of Pathology*, 161:1315-1323.

Gilbert, S. F. (2006). *Developmental Biology, Eighth Edition.* Sunderland, MA: Sinauer Associates Inc.

Guo, X., Day, T. F., Jiang, X., Garrett-Beal, L., Topol, L., & Yang, Y. (2004). Wnt/β-catenin signaling is sufficient and necessary for synovial joint formation. *Genes and Development*, 18:2404-2417.

Habas, R., & Dawid, I. B. (2005). Dishevelled and Wnt signalling: is the nucleus the final frontier? *Journal of Biology*, 4:2.

Hall, B. K., & Miyake, T. (1992). The membranous skeleton: the role of cell condensations in vertebrate skeletogenesis. *Anatomy and Embryology*, 186:107-124.

Handley, C. J., Samiric, T., & Ilic, M. Z. (2006). Structure, Metabloism, and Tissue Roles of Chondroitin Sulfate Proteoglycans. *Advances in Pharmacology*, 53:219-232.

Hartmann, C., & Tabin, C. J. (2000). Dual roles of Wnt signaling during chondrogenesis in the chicken limb. *Development*, 127, 3141-3159.

Harumoto, T., Ito, M., Shimada, Y., Kobayashi, T. J., Ueda, H. R., Lu, B., & Uemura, T. (2010). Atypical caherins Dachous and Fat control dynamics of noncentrosomal microtubules in planar cell polarity. *Developmental Cell*, 19:389-401.

Higuchi, R., Fockler, C., Dollinger, G., & Watson, R. (1993). Kinectic PCR analysis: real-time monitoring of DNA amplification reactions. *Biotechnology*, 11:1026-1030.

Hudson KS, A. K. (2010). Versican G1 domain and V3 isoform overexpression results in increased chondrogenesis in the developing chick in ovo. *The Anatomical Record* , 293: 1669-1678.

Huguet, E. L., McMahon, J. A., McMahon, A. P., Bickell, R., & Harris, A. L. (1994). Differential Expression of Human Wnt Genes 2, 3, 4, and 7B in Human Breast Cell Lines and Normal and Disease States of Human Breast Tissue. *American Association for Cancer Research*, 54:2615-2621.

Inoue, Y., Yoneda, M., Miyaishi, O., Iwaki, M., & Zako, M. (2009). Hyaluronan dynamics during retinal development. *Brain Research*, 1256:55-60.

Jefferies, S., Robbins, D. J., & Capobianco, A. J. (2002). Characterization of a High-Molecular-Weight Notch Complex in the Nucleus of NotchIC-Transformed RKE Cells and in a Human T-Cell Leukemia Cell Line. *Molecular and Cellular Biology*, 22:11:3927-3941.

Jiang, F., Parsons, C. J., & Stefanovic, B. (2006). Gene expression profile of quiescent and activated rat hepatic stellate cells implicates Wnt signaling pathway in activation. *Journal of Hepatology*, 45:401-409.

Kamiya N, W. H. (2006). Versican/PG-M regulates chondrogenesis as an extracellular matrix molecule crucial for mesenchymal condensation. *Journal of Biochemistry*, 281(4):2390-400.

Kawakami Y, W. N. (1999). Involvement of Wnt-5a in chondrogenic pattern formation in the chick limb bud. *Developmen, Growth and Differentiation*, 41(1):29-40.

Keller, R., Davidson, L. A., & Shook, D. R. (2003). How we are shaped: the biomechanics of gastrulation. *Differentiation*, 71:171-205.

Kimata K, O. Y. (1986). A large chondroitin sulfate proteoglycan (PG-M) synthesized before chondrogenesis in the limb bud of chick embryo. *Journal of Biochemistry*, 261(29):13517-25.

Komiya, Y., & Habas, R. (2008). Wnt signal transduction pathways. *Organogenesis*, 4(2):68-75.

Kornfield, R., & Kornfield, S. (1980). *The Biochemistry pf Glycoproteins.* New York: Plenum Press.

Laufer, E., Dahn, R., Orozco, O. E., Yeo, C. Y., Pistenti, J., Henrique, D., . . . Tabin, C. (1997). Expression of Radical fringe limb-bud ectoderm regulates apicl ectodermal ridge formation. *Nature*, 388(6640):400.

Lee, A.-K., Ahn, S.-G., Yoon, J.-H., & Kim, S.-A. (2011). Sox4 stimulates ß-catenin activity through induction of CK2. *Oncology Reports*, 25:559-565.

Lee, G. M., Johnstone, B., Jacobson, K., & Caterson, B. (1993). The Dynamic Structure of Pericelluar Matrix on Living Cell. *The Journal of Cell Biology*, 123:1899-1907.

Legg, J. W., Lewis, C. A., Parsons, M., Ng, T., & Isacke, C. M. (2002). A novel PKC-regulated mechanism controls CD44 exrin association and directional cell motility. *Nature Cell Biology*, 4:399-407.

Lepperdinger G, M. J. (2001). Hyal2--less active, but more versatile? *Matirx Biology* , 20(8):509-14.

Lepperdinger, G., Strobl, B., & Kreil, G. (1998). HYAL2, a Human Gene Expressed in Many Cells, Encodes a Lysosomal Hyaluronidase with a Novel Type of Specificity. *The Journal of Biological Chemistry*, 273:35:22466-22470.

Lesley, J., Hyman, R., & Kincade, P. W. (1993). CD44 and its interaction with extracellular matrix. *Advances in Immunology*, 54:271-335.

Loganathan PG, N. S. (2005). Comparative analysis of the expression patterns of Wnts during chick limb development. *Histochem Cell Biology*, 123(2):195-201.

Longpre, J.-M., McCulloch, D. R., Koo, B.-H., Alexander, J. P., Apte, S. S., & Leduc, R. (2009). Characterization of proADAMTS5 processing by proprotein convertases. *The International Journal of Biochemistry & Cell Biology*, 41(5):1116-1126.

Matsumoto K, S. M. (2003). Distinct interaction of versican/PG-M with hyaluronan and link protein. *Journal of Biochemistry*, 17;278(42):41205-12.

Medina, A., Reintsch, W., & Steinbeisser, H. (2000). Xenopus frizzled 7 can act in canonical and non-canonical Wnt signaling pathways: implications on early patterning and morphogenesis. *Mechanisms of Development*, 92:227-237.

Nagchowdhuri, P. S., Andrews, K. N., Robart, S., & Capehart, A. A. (2012). Versican Knockdown Reduces Interzone Area During Early Stages of Chick Synovial Joint Development. *The Anatomical Record*, 295:397-409.

Ng, L. J., Wheatly, S., Muscat, G. E., Conway-Campbell, J., Bowles, J., Wright, E., . . . Koopman, P. (1997). SOX9 Binds DNA, Activates Transcription, and Coexpresses with Type II Collagen during Chondrogenesis in the Mouse. *Developmental Biology*, 183:108-121.

Nolan, T., Hands, R. E., & Bustin, S. A. (2006). Quantification of mRNA using real-time RT-PCR. *Nature Protocols*, 1:1559-1582.

Ohuchi, H., Nakagawa, T., Yamamoto, A., Araga, A., Ohata, T., Ishimaru, Y., . . . Noji, S. (1997). The mesenchymal factor, FGF10, initiates and maintains the outgrowth of the chick limb bud through interaction with FGF8, an apical ectodermal factor. *Development*, 124:2235-2244.

Okamoto, I., Kawano , Y., Murakami, D., Sasayama, T., Araki, N., Miki, T., . . . Saya, H. (2001). Proteolytic release of CD44 intracellular domain and its role in the CD44 signaling pathway . *Journal of Cell Biology*, 155:755-762.

Pacifici M, K. E. (2005). Mechanisms of synovial joint and articular cartilage formation: recent advances, but many lingering mysteries. *Birth Defects Research* , 75(3):237-48.

Park, M., & Moon, R. (2002). The planar cell-polarity gene stbm regulates cell behaviour and cell fate in vertebrate embryos. *Nature Cell Biology*, 4:20-26.

Parr BA, M. A. (1995). Dorsalizing signal Wnt-7a required for normal polarity of D-V and A-P axes of mouse limb. *Nature*, 23;374(6520):350-3.

Perin, J.-P., Bonnet, F., Thurieau, C., & Jolles, P. (1987). Link Protein Interactions with Hyaluronate and Proteoglycans. *The Journal of Biological Chemistry*, 262:27:13269-13272.

Peterson, R. S., Andhare, R. A., Rousche, K. T., Knudson, W., Wang, W., Grossfield, J. B., . . . Knudson, C. B. (2004). CD44 modulates Smad1 activation in the BMP-7 signaling pathway. *The Journal of Cell Biology*, 166(7):1081-1091.

Pfaffl, M. W. (2001). A new mathematical model for relative quantification in real-time PCR. *Nucleic Acids Research*, 29:9:2002-2007.

Pitsillides, A. A., & Ashhurst, D. E. (2008). A Critical Evaluation of Specific Aspects of Joint Development. *Developmental Dynamics*, 237:2284-2294.

Rai, S. K., Duh, F.-M., Vigdorovich, V., Danilkovitch-Miagkova, A., Lerman, M. I., & Miller, A. D. (2001). Candidate tumor suppressor HYAL2 is a glycosylphosphatidylinositol (GPI)-anchored cell-surface receptor for jaagsiekte sheep retrovirus, the envelope protein of which mediates oncogenic transformation. *Proceedings of the National Academy of Sciences of the United States of America*, 98:8:4443-4448.

Rousche, K. T., & Knudson, C. B. (2002). Temporal expression of CD44 during embryonic chick limb development and modulation of its expression with retinoic acid. *Matrix Biology*, 53-62.

Seyfried, N. T., McVey, G. F., Almond, A., Mahoney, D. J., Dudhia, J., & Day, A. J. (2005). Expression and Purification of Functionally Active Hyaluronan-binding Domains from

Human Cartilage Link Protein, Aggrecan and Versican. *The Journal of Biological Chemistry*, 280:7:5435-5448.

Shaul, Y., & Ben-Yehoyada, M. (2005). Role of c-Abl in the DNA damage stress response. *Cell Research*, 15:1:33-35.

Shepard JB, K. H. (2007). Versican expression during synovial joint morphogenesis. *InternaTIONAL Journal of Biological Science*, 3(6):380-4.

Shepard, J. B., Gliga, D. A., Morrow, A. P., & Capehart, A. A. (2008). Versican knock-down compromises chondrogenesis in the embryonic chick limb. *Anatomical Record*, 291(1):19-27.

Shinomura, T., Jensen, K. L., Yamagata, M., Kimata, K., & Solursh, M. (1990). The distribution of mesenchyme proteoglycan (PG-M) during wing bud outgrowth. *Anatomy and Embryology*, 181:227-233.

Shinomura, T., Nishida, Y., Ito, K., & Kimata, K. (1993). cDNA Cloning of PG-M, a Large Chondroitin Sulfate Proteoglycan Expressed during Chondrogenesis in Chick Limb Buds. *The Journal of Biological Chemistry*, 268:19:14461-14469.

Sinner, D., Kordich, J. J., Spence, J. R., Opoka, R., Rankin, S., Lin, S. C., . . . Wells, J. M. (2007). Sox17 and Sox4 differentially regulate β-catenin/T-cell factor activity and proliferation of colon carcinoma cells. *Molecular Cell Biology*, 27:7802-7815.

Snow HE, R. L. (2005). Versican expression during skeletal/joint morphogenesis and patterning of muscle and nerve in the embryonic mouse limb. *The Anatomical Record Part A*, 282(2):95-105.

Spicer, A. P., Kaback, L. A., Smith, T. J., & Seldin, M. F. (1998). Molecular Cloning and Characterization of the Human and Mouse UDP-Glucose Dehydrogenase Genes. *The Journal of Biological Chemistry*, 273:39:25117-25124.

Stark, K., Vainio, S., Vassileva, G., & McMahon, A. P. (1994). Epithelial transformation of metanephric mesenchyme in the developing kidney regulated by Wnt-4. *Nature*, 327:679-683.

Storm, E. E., & Kingsley, D. M. (1999). GDF-5 coordinates bone and joint formation during digit development. *Developmental Biology*, 11-27.

Tien , J. Y., & Spicer, A. P. (2005). Three Vertebrate Hyaluronan Synthases Are Expressed During Mouse Development in Distinct Spatial and Temporal Patterns. *Developmental Dynamics*, 233:103-141.

Towers M, T. C. (2009). Growing models of vertebrate limb development. *Development*, 136(2):179-90.

Vincent, S., Luis-Ravelo, D., Anton, I., Garcia-Tunon, I., Borras-Cuesta, F., Dotor, J., . . . Lecanda, F. (2008). A Novel Lung Cancer Signature Mediates Metastatic Bone Colonization by a Dual Mechanism. *American Association for Cancer Research*, 68:2275–2285.

Wallingford, J. B., Vogeli, K. M., & Harland, R. M. (2001). Regulation of convergent extension in Xenopus by Wnt5a and Frizzled-8 is independent of the canonical Wnt pathway. *International Journal of Development Biology*, 45:225-227.

Wegner, M. (1999). From head to toes: the multiple facets of Sox proteins. . *Nucleic Acids Research*, 27:1409-1420.

Wight, T. N. (2002). Versican: a versatile extracellular matrix proteoglycan in cell biology. *Current Opinion in Cell Biology*, 14:617-623.

Williams DR Jr, P. A. (2005). Limb chondrogenesis is compromised in the versican deficient hdf mouse. *Biomedical and Biophysical Research Communications*, 334(3):960-6.

Yang, B. L., Zhang, Y., Cao, L., & Yang, B. B. (1999). Cell Adhesion and Proliferation Mediated Through the G1 Domain of Versican. *Journal of Cellular Biochemistry*, 72:210-220.

Zhang, Y., Cao, L., Kiani, C., Yang, B. L., Hu, W., & Yang, B. B. (1999). Promotion of Chondrocyte Proliferation by Versican Mediated by G1 Domain and EGF-like Motifs. *Journal of Cellular Biochemistry*, 73:445-457.

Zhang, Y., Cao, L., Yang, B. L., & Yang, B. B. (1998). The G3 Domain of Versican Enhances Cell Proliferation via Epidermial Growth Factor-like Motifs. *The Journal of Biological Chemistry*, 273:33:21342-21351.

Zhao, C., Aviles, C., Abel, R. A., Almli, C. R., McQuillen, P., & Pleasure, S. J. (2005). Hippocampal and visuospatial learning defects in mice with a deletion of frizzled 9, a gene in the Williams syndrome deletion interval. *Development and disease*, 132:2917-2927.

Zimmermann DR, R. E. (1989). Multiple domains of the large fibroblast proteoglycan, versican. *EMBO Journal*, (10):2975-81.

Appendix A. Animal Care and Use Committee Form.

East Carolina University

Animal Care and Use Commitee
212 Ed Warren Life Sciences Building
East Carolina University
Greenville, NC 27834

252-744-2436 office
252-744-2355 fax

February 14, 2011

Anthony Capehart, Ph.D.
Department of Biology
Howell Science Complex
East Carolina University

Dear Dr. Capehart:

Your Animal Use Protocol entitled, "Hyaluronidase, a Hydrolase that Contributes to the Formation of Limb Joints during Embryonic Development and the Destruction of Joints in Adults with Osteoarthritis" (AUP #D258) was reviewed by this institution's Animal Care and Use Committee on 2/14/11. The following action was taken by the Committee:

"Approved as submitted"

Please contact Dale Aycock at 744-2997 prior to hazard use

A copy is enclosed for your laboratory files. Please be reminded that all animal procedures must be conducted as described in the approved Animal Use Protocol. Modifications of these procedures cannot be performed without prior approval of the ACUC. The Animal Welfare Act and Public Health Service Guidelines require the ACUC to suspend activities not in accordance with approved procedures and report such activities to the responsible University Official (Vice Chancellor for Health Sciences or Vice Chancellor for Academic Affairs) and appropriate federal Agencies.

Sincerely yours,

Scott E. Gordon, Ph.D.
Chairman, Animal Care and Use Committee

SEG/jd

enclosure

Appendix B. Fold Change results from initial real-time PCR experiment when Versican was knocked down.

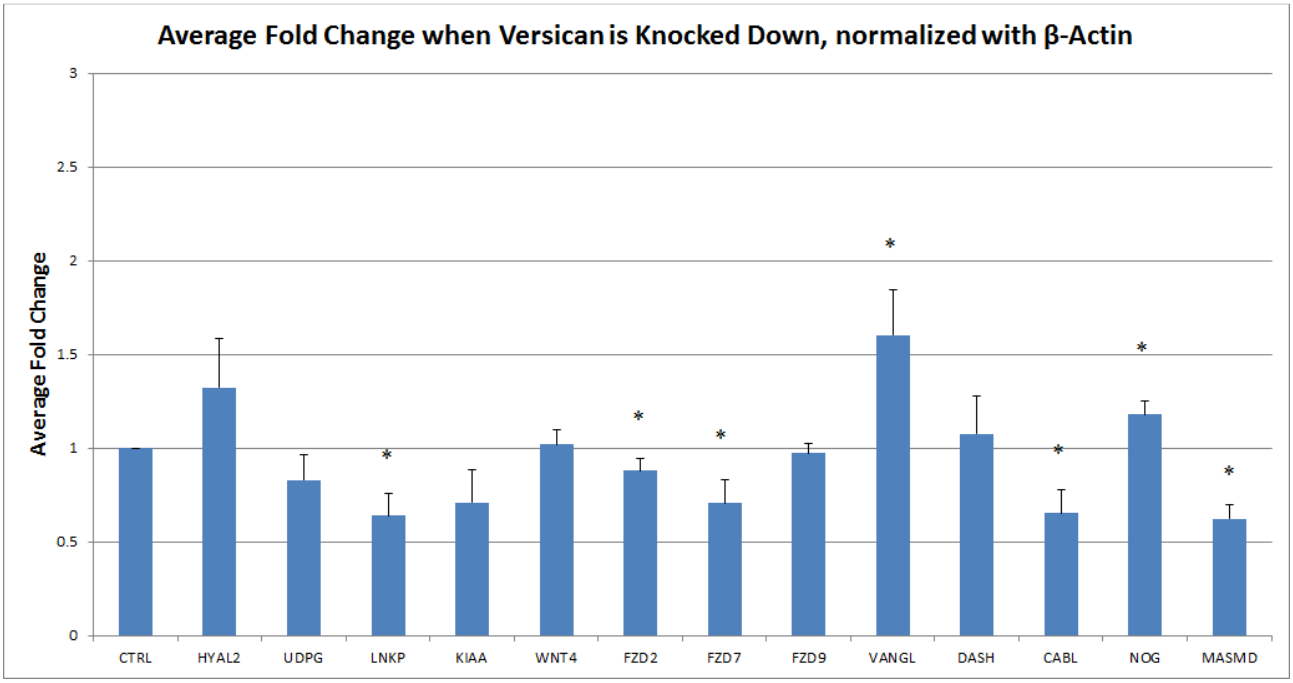

Appendix B. Average fold changes from real-time PCR using template cDNA samples in which versican has been knockdown. Bars denote standard error of the mean and asterisks denote significance at $p < 0.05$.

Appendix C. In Situ Hybridization Primer Pairs.

Gene Name	Accession #	F. Primer: 5'-3'	R. Primer: 5'-3'	Sequence Length
CABL	XM_422269	ATTGTGGGCACGGTCCTTTCC	GCTGCTCTCACTCTCACGAACC	495
Dachsous	XM_417264	CACTGGTGCTCTCTCTGTTG	CAGGGTCAGTGGCACGCAGG	542
Frizzled 2	NM_204222	CGGCCACATGTTCTTCAACGAGG	TGAGCCCCACGAAGCAGACG	527
Frizzled 8	XM_426568	GCATCCGCAGCGTGATCAAG	TCACACATGGGACAGCGGGAC	443
Frizzled 9	AF224319	TGCTCACCTTCCTGCTCGACCC	AAAGACAGCCACGGTGGGCAC	776
HYAL 2	XM_414258	CCGACTGCTACAACCACGAC	CAGGAAGACATTGGCGGTGC	536
Link Protein	NM_205482	GACACCACAGAAAGAGCTAC	GCTTGGTTGGGTGTATTAGG	513
UDPGDH	NM_001012581	CTGTATCGGTGCTGGCTATG	GCTGCCTCCAAACCCAACAC	802
Wnt4	NM_204783	CTCACAGTCCTTTGTCGACG	CCCGATGGCAGGGTTTGCAC	536

Appendix C. Successful primer pairs originally designed for probe designed for *in situ* hybridization.